ANTENNA LABORATORY REPORT NO. 72-3

CURRENT DISTRIBUTION ON A CYLINDRICAL ANTENNA WITH PARALLEL ORIENTATION IN A LOSSY MAGNETOPLASMA

BY

C. A. KLEIN, P. W. KLOCK, AND G. A. DESCHAMPS

SCIENTIFIC REPORT NO. 19

JULY 1972

SPONSORED BY

NATIONAL AERONAUTICS AND SPACE ADMINISTRATION

NGR-14-005-009

ANTENNA LABORATORY
DEPARTMENT OF ELECTRICAL ENGINEERING
ENGINEERING EXPERIMENT STATION
UNIVERSITY OF ILLINOIS
URBANA, ILLINOIS 61801

UILU-ENG-72-2546

ANTENNA LABORATORY REPORT NO. 72-3

CURRENT DISTRIBUTION ON A CYLINDRICAL ANTENNA WITH PARALLEL ORIENTATION IN A LOSSY MAGNETOPLASMA

BY

C. A. KLEIN, P. W. KLOCK, AND G. A. DESCHAMPS

SCIENTIFIC REPORT NO. 19

JULY 1972

SPONSORED BY

NATIONAL AERONAUTICS AND SPACE ADMINISTRATION

NGR-14-005-009

ANTENNA LABORATORY
DEPARTMENT OF ELECTRICAL ENGINEERING
ENGINEERING EXPERIMENT STATION
UNIVERSITY OF ILLINOIS
URBANA, ILLINOIS 61801

ABSTRACT

The current distribution and impedance of a thin cylindrical antenna with parallel orientation to the static magnetic field of a lossy magnetoplasma is calculated with the method of moments. The electric field produced by an infinitesimal current source is first derived. Results are presented for a wide range of plasma parameters. Reasonable answers are obtained for all cases except for the overdense hyperbolic case. A discussion of the numerical stability is included which not only applies to this problem but other applications of the method of moments.

TABLE OF CONTENTS

LIST OF TABLES

LIST OF FIGURES

CHAPTER I. INTRODUCTION

Since man has launched space vehicles into the ionosphere, there has been strong interest in the effect of plasmas on antennas. A primary interest is understanding the effects of the plasma on the current distribution and the antenna impedance. Since cylindrical antennas have a simple geometry, are well-understood in free space, and have wide usage, they are most commonly studied in plasma problems. Because one cannot analytically solve Maxwell's equations for a lossy magnetoplasma with cylindrical boundary conditions, a current distribution usually is assumed. This assumed current distribution, though, represents only the limiting case of an infinitesimal antenna. Approximations made by other workers give results valid for infinite length antennas. These approximations simplify the analytical work but give results of questionable validity for the finite antenna.

The approach used in this report eliminates these approximations. The method of moments is used to solve for current distribution on the antenna. Basically, this method converts an integral equation into a matrix equation which can be easily solved by computer methods. From the current distribution one can trivially find the impedance at the feed point. Thus, the current distribution and impedance for the finite antenna over a wide range of plasma densities and applied magnetic fields can be calculated.

The geometry used in this problem is shown in Figure 1. The orientation of the antenna is restricted to the z direction parallel to the applied magnetic field. The antenna is described by the half-length H and radius a. For a thin-wire antenna, the condition $a \ll H$

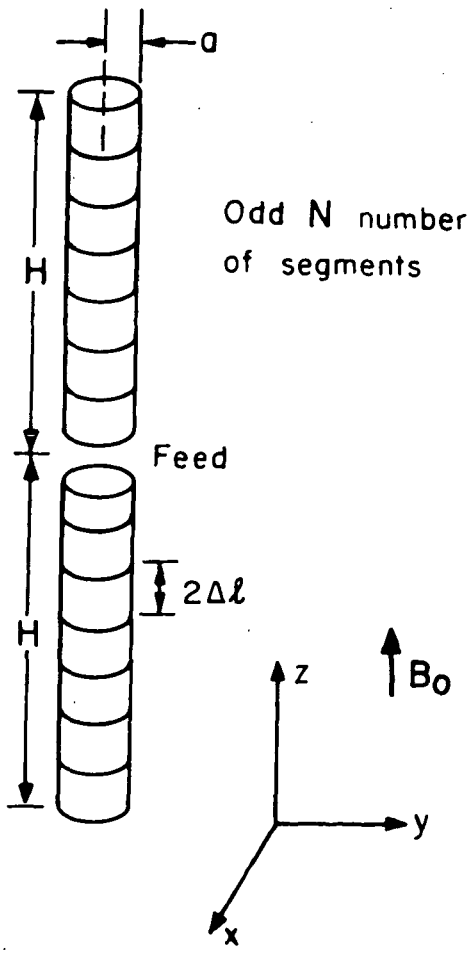

Figure 1. Geometry of Problem

must hold. For the method of moments, the antenna is divided into an odd number of segments N.

The first step in applying the method of moments is solving for the electric field due to an infinitesimal source. Exact details of how the method of moments is applied will be discussed. Results are given for a wide range of plasma parameters and are compared to the limiting cases of free space and quasi-static models. Comparisons are also made to experimental data. A sensitivity theory is discussed which applies not only to this problem but to many other applications of the moment method.

CHAPTER II. FIELDS DUE TO INFINITESIMAL SOURCE

2.0 An Overview

To determine the current distribution along an antenna it is first necessary to find the fields produced by an infinitesimal current source. The derivation given here used the notation and technique developed by Mittra and Deschamps [1]. In their paper they outline the derivation of the field components for any orientation of an infinitesimal source. The parallel orientation case worked out in detail here, however, is not the same as the specific case completed in their paper.

In this report the plasma will be characterized by normalized plasma parameters X, Y, and Z where

$$X = \left(\frac{\omega_p}{\omega}\right)^2, \quad Y^2 = \left(\frac{\omega_c}{\omega}\right)^2, \quad Z = \frac{\nu}{\omega}$$

$$\omega_p = \left[\frac{N_o e^2}{m\varepsilon_o}\right]^{1/2} = \text{plasma frequency} \qquad (2.1)$$

$$\omega_c = \frac{eB_o}{m} = \text{cyclotron frequency}$$

ω = operating frequency

ν = collision frequency

N_o = average electron density

e = magnitude of electronic charge

m = mass of electron

B_o = applied magnetic field.

The use of X, Y, and Z parameters allows one to indicate results on commonly used plasma diagrams.

Before giving the lengthy details, we wish to give an overview of the derivation. Maxwell's equations can be combined to yield a relation for the electric field caused by an infinitesimal source in the plasma. Taking the Fourier transform allows one to easily solve for the transform of the z component of the electric field. The main feature of this technique is that in performing the inverse Fourier transform, the integral can be broken into a sum of functions such that one can analytically integrate terms that are singular when observation and source points coincide. These terms represent the near field and are dominant in the determination of the antenna current and impedance. Terms that are finite when observation and source points coincide need to be numerically integrated, but these represent far-field terms and need not be as accurate because of their small relative size. The rest of this chapter gives the details; the final expressions for the field due to the infinitesimal source are given by Equations (2.80) through (2.88).

2.1 Maxwell's Equations

Using $e^{j\omega t}$ time convention, Maxwell's equations for the plasma are

$$\text{curl } \bar{E} = -j\omega\mu\bar{H} \tag{2.2a}$$

$$\text{curl } \bar{H} = j\omega\varepsilon_o \bar{\bar{\varepsilon}} \cdot \bar{E} + \bar{J} \tag{2.2b}$$

$$\text{div } \bar{H} = 0 \tag{2.2c}$$

$$\text{div } \bar{\bar{\varepsilon}} \cdot \bar{E} = \rho/\varepsilon_o \tag{2.2d}$$

where

$$\overline{\overline{\varepsilon}} = \begin{bmatrix} \varepsilon & -j\varepsilon' & 0 \\ j\varepsilon' & \varepsilon & 0 \\ 0 & 0 & \varepsilon_z \end{bmatrix} \tag{2.3}$$

$$U = 1 - jZ$$

$$\varepsilon = 1 - UX/(U^2 - Y^2)$$

$$\varepsilon' = \frac{YX}{U^2 - Y^2}$$

$$\varepsilon_z = 1 - X/U.$$

When (2.2a) and (2.2b) are combined, the following equation is obtained

$$\text{curl curl } \overline{E} = k_o^2 \overline{\overline{\varepsilon}} \cdot \overline{E} - j\omega\mu\overline{J}, \quad k_o^2 = \omega^2\mu\varepsilon_o. \tag{2.4}$$

At this point it becomes convenient to transform the problem into k-space by applying the Fourier transform. Let $\overline{E}'$ and $\overline{J}'$ represent the transforms of $\overline{E}$ and $\overline{J}$. The transform E_x' of E_x is defined by

$$E_x'(k_x, k_y, k_z) = \int_{-\infty}^{\infty}\int\int E_x(x, y, z)\, e^{j(k_x x + k_y y + k_z z)}\, dxdydz \tag{2.5}$$

with the transforms of other components defined similarly. Note that the del operator can be replaced by $j\overline{k}$. Then, using a vector identity, the transform of (2.4) can be written as

$$\overline{k}(\overline{k} \cdot \overline{E}') - \overline{k} \cdot \overline{k}\, \overline{E}' + k_o^2 \overline{\overline{\varepsilon}}\, \overline{E}' = j\omega\mu\overline{J}'. \tag{2.6}$$

Next one can expand this equation by components and write it in matrix

form

$$\left\{ -k_o^2 \begin{bmatrix} \varepsilon & -j\varepsilon' & 0 \\ j\varepsilon' & \varepsilon & 0 \\ 0 & 0 & \varepsilon_z \end{bmatrix} - \begin{bmatrix} -k_y^2-k_z^2 & k_x k_y & k_x k_z \\ k_x k_y & -k_x^2-k_z^2 & k_y k_z \\ k_x k_z & k_y k_z & -k_x^2-k_y^2 \end{bmatrix} \right\} \begin{bmatrix} E'_x \\ E'_y \\ E'_z \end{bmatrix} = -j\omega\mu \begin{bmatrix} J'_x \\ J'_y \\ J'_z \end{bmatrix} . \tag{2.7}$$

Because of the radial symmetry about the z axis, $\bar{k}$ can be represented by spherical coordinates (Γ, Ψ, α),

$$k_x = \Gamma \sin\Psi\cos\alpha, \quad k_y = \Gamma \sin\Psi \sin\alpha, \quad k_z = \Gamma \cos\Psi. \tag{2.8}$$

Making these changes and collecting terms, we obtain

$$M\bar{E}' = j \frac{\eta}{k_o} \bar{J}' \tag{2.9}$$

$$M = \begin{bmatrix} \varepsilon-\Gamma_1^2(1 - \sin^2\Psi \cos^2\alpha) & -j\varepsilon'+\Gamma_1^2 \sin^2\Psi \sin\alpha \cos\alpha & \Gamma_1^2 \sin\Psi \cos\Psi \cos\alpha \\ j\varepsilon'+\Gamma_1^2 \sin^2\Psi \sin\alpha \cos\alpha & \varepsilon-\Gamma_1^2(1 - \sin^2\Psi \sin^2\alpha) & \Gamma_1^2 \sin\Psi \cos\Psi \sin\alpha \\ \Gamma_1^2 \sin\Psi \cos\Psi \cos\alpha & \Gamma_1^2 \sin\Psi \cos\Psi \sin\alpha & \varepsilon_z - \Gamma_1^2 \sin^2\Psi \end{bmatrix}$$

where $\Gamma_1 = \Gamma/k_o$.

To solve for $\bar{E}'$ we can write

$$\bar{E}' = M^{-1} j \frac{\eta}{k_o} \bar{J}'. \tag{2.10}$$

Finding M^{-1} is a straightforward but lengthy algebraic manipulation. One finally obtains

$$M^{-1} = [a_{ij}]/\Delta \tag{2.11}$$

$$\Delta = \det(M) = \Gamma_1^4(\varepsilon \sin^2\Psi + \varepsilon_z \cos^2\Psi) - \Gamma_1^2[\varepsilon\,\varepsilon_z(1 + \cos^2\Psi) + (\varepsilon^2 - \varepsilon'^2)\sin^2\Psi] + (\varepsilon^2 - \varepsilon'^2)\varepsilon_z$$

$$a_{11} = \Gamma_1^4 \sin^2\Psi \cos^2\alpha - \Gamma_1^2[\varepsilon \sin^2\Psi + \varepsilon_z(1 - \sin^2\Psi \sin^2\alpha)] + \varepsilon\,\varepsilon_z$$

$$a_{21} = \Gamma_1^4 \sin^2\Psi \sin\alpha \cos\alpha - \Gamma_1^2 \sin^2\Psi(\varepsilon_z \sin\alpha \cos\alpha - j\varepsilon') - j\varepsilon'\,\varepsilon_z$$

$$a_{31} = \Gamma_1^2 \sin\Psi \cos\Psi\,[\Gamma_1^2 \cos\alpha - (\varepsilon \cos\alpha - j\varepsilon' \sin\alpha)]$$

$$a_{12} = \Gamma_1^4 \sin^2\Psi \sin\alpha \cos\alpha - \Gamma_1^2 \sin^2\Psi\,(\varepsilon_z \sin\alpha \cos\alpha + j\varepsilon') + j\varepsilon'\,\varepsilon_z$$

$$a_{22} = \Gamma_1^4 \sin^2\Psi \sin^2\alpha - \Gamma_1^2[\varepsilon \sin^2\Psi + \varepsilon_z\,(1 - \sin^2\Psi \cos^2\alpha)] + \varepsilon\,\varepsilon_z$$

$$a_{32} = \Gamma_1^2 \sin\Psi \cos\Psi\,[\Gamma_1^2 \sin\alpha - (\varepsilon \sin\alpha + j\varepsilon' \cos\alpha)]$$

$$a_{13} = \Gamma_1^2 \sin\Psi \cos\Psi\,[\Gamma_1^2 \cos\alpha - (\varepsilon \cos\alpha + j\varepsilon' \sin\alpha)]$$

$$a_{23} = \Gamma_1^2 \sin\Psi \cos\Psi\,[\Gamma_1^2 \sin\alpha - (\varepsilon \sin\alpha - j\varepsilon' \cos\alpha)]$$

$$a_{33} = \Gamma_1^4 \cos^2\Psi - \Gamma_1^2\,\varepsilon(1 + \cos^2\Psi) + \varepsilon^2 - \varepsilon'^2$$

where $\Gamma_1 = \Gamma/k_o$.

It should be noted that $\det(M) = 0$ is the dispersion relation for the plasma. Since, for a fixed polar angle Ψ, this is a second-degree polynomial in Γ_1^2, there will be exactly two roots. These two roots are the squares of the indices of refraction for two characteristic plane waves traveling at an angle Ψ to the magnetic field. The proper square root must be taken to satisfy the radiation condition. One can appreciate

the conceptual difficulties inherent in understanding plasma problems since unlike free space, there is not even a unique wavelength in a given direction. The exact form of the indices of refraction will be given shortly.

To solve our problem, only one of the nine terms of (2.11) will be needed. For parallel orientation of the antenna, there is only source current in the z direction. Only E_z' is constrained by the boundary condition. Therefore, the rest of this chapter is directed to finding the inverse transform of

$$E_z' = (a_{33}/\Delta)\,\frac{j\eta}{k_o}\,J_z' \,. \tag{2.12}$$

2.2 Inverse Transform

Conceptually all that remains is to perform the inverse transform

$$E_z(x, y, z) = \frac{j\eta}{k_o}\left(\frac{1}{2\pi}\right)^3 \int\int\int_{-\infty}^{\infty} \left(\frac{a_{33}}{\Delta}\right) e^{-j\bar{k}\cdot\bar{r}}\, d\bar{k}. \tag{2.13}$$

Recall that J_z' is unity since our problem is formulated for a Dirac δ source. If spherical coordinates are also used for the observation point, (2.13) becomes

$$E_z(R, \theta, \phi) = \frac{j\eta}{k_o}\left(\frac{1}{2\pi}\right)^3 \int_0^{\infty}\int_0^{\pi}\int_0^{2\pi} \left(\frac{a_{33}}{\Delta}\right) e^{-j\Gamma R[\sin\theta\sin\Psi\cos(\alpha-\phi)+\cos\theta\cos\Psi]}$$

$$\cdot\, \Gamma^2 \sin\Psi\, d\alpha\, d\Psi\, d\Gamma$$

where $x = R\sin\theta\cos\Psi$, $y = R\sin\theta\sin\phi$, $z = R\cos\theta$.

First we can relatively easily perform the α integration using the following standard integration formula [2].

$$J_o(\Gamma R \sin\theta \sin\Psi) = \frac{1}{2\pi}\int_0^{2\pi} e^{-j\Gamma R \sin\theta \sin\Psi \cos(\alpha-\phi)}\, d\alpha. \qquad (2.15)$$

Applying (2.15) to (2.14) produces

$$E_z = \frac{j\eta}{k_o}\left(\frac{1}{2\pi}\right)^2 \int_0^{\infty}\int_0^{\pi} \left(\frac{a_{33}}{\Delta}\right) J_o(\Gamma R \sin\theta \sin\Psi)\, e^{-jR\cos\theta\cos\Psi}\, \Gamma^2 \sin\Psi\, d\Psi\, d\Gamma \qquad (2.16)$$

$$\frac{a_{33}}{\Delta} = \frac{\Gamma_1^4\cos^2\Psi - \Gamma_1^2\,\varepsilon(1+\cos^2\Psi) + \varepsilon^2 - \varepsilon'^2}{\Gamma_1^4(\varepsilon\sin^2\Psi + \varepsilon_z\cos^2\Psi) - \Gamma_1^2[\varepsilon\,\varepsilon_z(1+\cos^2\Psi) + (\varepsilon^2 - \varepsilon'^2\sin^2\Psi] + (\varepsilon^2-\varepsilon'^2)\varepsilon_z}$$

$$\Gamma_1 = \Gamma/k_o .$$

At this point it is convenient to write Δ in factored form.

$$\Delta(\Gamma, \Psi) = (\varepsilon \sin^2\Psi + \varepsilon_z \cos^2\Psi)(\Gamma_1^2 - n_1^2)(\Gamma_1^2 - n_2^2) \qquad (2.17)$$

where

$$n_1^2,\ n_2^2 = \frac{B(\Psi) \pm \sqrt{B^2(\Psi) - 4A(\Psi)\,C(\Psi)}}{2A(\Psi)}$$

$$A(\Psi) = \varepsilon \sin^2\Psi + \varepsilon_z \cos^2\Psi$$

$$B(\Psi) = \varepsilon\,\varepsilon_z(1+\cos^2\Psi) + (\varepsilon^2 - \varepsilon'^2)\sin^2\Psi$$

$$C(\Psi) = (\varepsilon^2 - \varepsilon'^2)\,\varepsilon_z .$$

Recall n_1 and n_2 represent indices of refraction in the plasma mentioned earlier.

The ability to do the integration in (2.16) depends upon it being possible to break $\frac{a_{33}}{\Delta}$ into a sum of functions with different dominant orders of Γ. As mentioned in the overview, it will be shown that those terms which are singular when observation and source point coincide can

be integrated in closed form. These represent near-field terms and will be dominant in this problem. Those terms that are finite when observation and source points coincide will need to be integrated numerically but will be small compared to singular terms.

By successive synthetic division one can show

$$\frac{a_{33}}{\Delta}\Gamma^2 = \frac{\cos^2\Psi\,\Gamma^2}{A(\Psi)} + \frac{k_o^2(\varepsilon^2 + \varepsilon'^2\cos^2\Psi)\sin^2\Psi}{A^2(\Psi)} \tag{2.18}$$

$$- k_o^2\sin^2\Psi\,\frac{\{\Gamma^2k_o^2[\varepsilon(\varepsilon^2-\varepsilon'^2) - (n_1^2+n_2^2)(\varepsilon^2+\varepsilon'^2\cos^2\Psi)] + n_1^2n_2^2(\varepsilon^2+\varepsilon'^2\cos^2\Psi)k_o^4\}}{(\Gamma^2 - n_1^2k_o^2)(\Gamma^2 - n_2^2k_o^2)A^2(\Psi)}$$

where $A(\Psi) = \varepsilon\sin^2\Psi + \varepsilon_z\cos^2\Psi$.

Let the various parts of the z component of the field be defined as follows

$$E_{zs} = \frac{j\eta}{k_o}\left(\frac{1}{2\pi}\right)^2\int_0^\infty\int_0^\pi \frac{\cos^2\Psi\,\Gamma^2}{\varepsilon\sin^2\Psi + \varepsilon_z\cos^2\Psi} J_o(\Gamma R\sin\theta\sin\Psi) \tag{2.19}$$

$$\cdot\, e^{-j\Gamma R\cos\theta\cos\Psi}\sin\Psi\,d\Psi d\Gamma.$$

$$E_{zfs} = -j\eta k_o\left(\frac{1}{2\pi}\right)^2\int_0^\infty\int_0^\pi \frac{(\varepsilon^2 + \varepsilon'^2\cos^2\Psi)\sin^3\Psi}{A^2(\Psi)} e^{-j\Gamma R\cos\theta\cos\Psi} \tag{2.20}$$

$$\cdot\, J_o(\Gamma R\sin\theta\sin\Psi)\,d\Psi d\Gamma$$

$$E_{zf} = j\eta k_o\left(\frac{1}{2\pi}\right)^2\int_0^\infty\int_0^\pi \frac{\sin^2\Psi\{\Gamma^2k_o^2[\varepsilon(\varepsilon^2-\varepsilon'^2)-(n_1^2+n_2^2)(\varepsilon^2+\varepsilon'^2\cos^2\Psi)]+n_1^2n_2^2(\varepsilon^2+\varepsilon'^2\cos^2\Psi)k_o^4\}}{(\Gamma^2 - n_1^2k_o^2)(\Gamma^2 - n_2^2k_o^2)\,A^2(\Psi)} \tag{2.21}$$

$$\cdot\, J_o(\Gamma R\sin\theta\sin\Psi)\, e^{-j\Gamma R\cos\theta\cos\Psi}\sin\Psi\,d\Psi d\Gamma.$$

The total field is given by

$$E_z = E_{zs} + E_{zfs} + E_{zf}. \tag{2.22}$$

When the total field is decomposed in this way, E_{zs} represents the most singular term in R, E_{zfs} the next most singular term, and E_{zf} represents a finite term. What remains now is the evaluation of each integral separately.

2.3 Integrating E_{zs}

The convergence of (2.19), the equation which defines E_{zs}, at first appears to be questionable. One can note that for a three-dimensional Fourier transform, ∇^2 with respect to the observation coordinates R and θ, can be replaced by $-\Gamma^2$. Therefore, (2.19) can be written as

$$E_{zs} = \frac{-j\eta}{k_o} \left(\frac{1}{2\pi} \right)^2 \nabla^2 I_s(R, \theta) \tag{2.23}$$

$$\nabla^2 I_s(R, \theta) = -\int_0^{\infty} \int_0^{\pi} \frac{\Gamma^2 \cos^2\Psi \sin\Psi}{\varepsilon \sin^2\Psi + \varepsilon_z \cos^2\Psi} e^{-j\Gamma R \cos\Psi \cos\theta} J_o(\Gamma R \sin\Psi \sin\theta) d\Gamma d\Psi \tag{2.24}$$

where the order of integration and differentiation has been formally interchanged.

Suppose we make the following change of variables to cylindrical coordinates.

$$\begin{aligned} z &= R \cos\theta, \quad \rho = R \sin\theta \\ \gamma &= \Gamma \cos\Psi, \quad u = \Gamma \sin\Psi \ . \end{aligned} \tag{2.25}$$

Then we can write (2.24)

$$\nabla^2 I_s(R, \theta) = \frac{1}{\rho} \frac{\partial}{\partial\rho} \rho \frac{\partial}{\partial\rho} \int_0^{\infty} \int_0^{\pi} \frac{\cos^2\Psi / \sin\Psi}{\varepsilon \sin^2\Psi + \varepsilon_z \cos^2\Psi} e^{-j\gamma z} J_o(u\rho) \, d\Psi d\Gamma \tag{2.26}$$

where Bessel's equation has been used to explicitly perform differentiation with respect to ρ outside the integral.

Completing the change of variable gives

$$\nabla^2 I_s(\rho, z) = \frac{1}{\rho}\frac{\partial}{\partial\rho}\rho\frac{\partial}{\partial\rho}\int_{u=0}^{\infty}\int_{\gamma=-\infty}^{\infty}\frac{\gamma^2 e^{-j\gamma z}}{u(\varepsilon u^2 + \varepsilon_z\gamma^2)} J_o(u\rho)\, d\gamma du. \tag{2.27}$$

First, to perform the γ integration, we will perform the integral

$$J = \int_{-\infty}^{\infty}\frac{\gamma^2 e^{-j\gamma z}}{\varepsilon u^2 + \varepsilon_z\gamma^2} d\gamma. \tag{2.28}$$

At this point we can explicitly change the order of differentiation with respect to z and the integration, thus completing the formal interchange indicated earlier.

$$J = \frac{-\partial^2}{\partial z^2}\int_{-\infty}^{\infty}\frac{e^{-j\gamma z}}{\varepsilon u^2 + \varepsilon_z\gamma^2} d\gamma. \tag{2.29}$$

At last we have an integration that can be performed with the aid of the residue theorem of complex variables. The integrand in Equation (2.29) is of exponential order; and therefore, for positive z we may close the integration path over the lower-half complex γ plane. There is only one simple pole at

$$\gamma = -j\sqrt{\varepsilon/\varepsilon_z}\,u .$$

One obtains

$$J = \frac{-\partial^2}{\partial z^2}\frac{\pi}{\sqrt{\varepsilon_z}}\frac{e^{-\sqrt{\varepsilon/\varepsilon_z}\,zu}}{\sqrt{\varepsilon}\,u} . \tag{2.30}$$

We substitute into (2.27) and perform differentiation with respect to z

$$\nabla^2 I_s = \frac{-\pi\sqrt{\varepsilon}}{\sqrt{\varepsilon_z^3}}\frac{1}{\rho}\frac{\partial}{\partial\rho}\rho\frac{\partial}{\partial\rho}\int_0^{\infty} e^{-\sqrt{\varepsilon/\varepsilon_z}\,zu} J_o(\rho u)\, du. \tag{2.31}$$

This final integration for E_{zs} can be performed to obtain

$$\nabla^2 I_s = \frac{-\pi\sqrt{\varepsilon}}{\sqrt{\varepsilon_z^3}} \frac{1}{\rho} \frac{\partial}{\partial\rho} \rho \frac{\partial}{\partial\rho} \frac{1}{\sqrt{\varepsilon z^2 + \varepsilon_z \rho^2}} \tag{2.32}$$

where the following definite integral has been used [3].

$$\int_0^\infty e^{-at} J_o(bt)\, dt = \frac{1}{\sqrt{a^2 + b^2}}. \tag{2.33}$$

Finally

$$E_{zs} = \frac{j\eta\sqrt{\varepsilon}}{4\pi k_o \varepsilon_z} \frac{1}{\rho} \frac{\partial}{\partial\rho} \rho \frac{\partial}{\partial\rho} \frac{1}{\sqrt{\varepsilon z^2 + \varepsilon_z \rho^2}} \tag{2.34}$$

or

$$E_{zs} = \frac{-j\eta\sqrt{\varepsilon}}{4\pi k_o \varepsilon_z} \frac{1}{(\varepsilon z^2 + \varepsilon_z \rho^2)^{3/2}} \left[\frac{2\varepsilon z^2 - \varepsilon_z \rho^2}{\varepsilon z^2 + \varepsilon_z \rho^2} \right]. \tag{2.35}$$

The dependence on distance can be seen more clearly by noting that $R' = \sqrt{\varepsilon}\sqrt{\varepsilon z^2 + \varepsilon_z \rho^2}$ is used as a plasma-scaled distance in some statics problems. Clearly

$$E_{zs} = \frac{-j\eta\varepsilon^2}{4\pi k_o \varepsilon_z} \cdot \frac{1}{R'^3} \cdot \left[\frac{2\varepsilon z^2 - \varepsilon_z \rho^2}{\varepsilon z^2 + \varepsilon_z \rho^2} \right]. \tag{2.35a}$$

2.4 Integrating E_{zfs}

We repeat (2.20), which defines E_{zfs},

$$E_{zfs} = -j\eta k_o \left(\frac{1}{2\pi} \right)^2 \int_0^\infty \int_0^\pi \frac{(\varepsilon^2 + \varepsilon'^2 \cos^2\Psi)\sin^3\Psi}{A^2(\Psi)} e^{-j\Gamma R \cos\theta \cos\Psi} \cdot J_o(\Gamma R \sin\theta \sin\Psi)\, d\Gamma d\Psi$$

$$A(\Psi) = \varepsilon \sin^2\Psi + \varepsilon_z \cos^2\Psi.$$

This term will be artificially divided into two terms E_{zfs1} and E_{zfs2} for ease of integration.

$$E_{zfs1} = -j\eta k_o \left(\frac{1}{2\pi}\right)^2 \varepsilon^2 I_{fs1} \tag{2.36}$$

where

$$I_{fs1} = \int_0^{\infty} \int_0^{\pi} \frac{\sin^3\Psi}{A^2(\Psi)} e^{-j\Gamma R \cos\theta \cos\Psi} \cdot J_o(\Gamma R \sin\theta \sin\Psi)\, d\Psi d\Gamma. \tag{2.37}$$

$$E_{zfs2} = -j\eta k_o \left(\frac{1}{2\pi}\right)^2 \varepsilon'^2 I_{fs2} \tag{2.38}$$

where

$$I_{fs2} = \int_0^{\infty} \int_0^{\pi} \frac{\cos^2\Psi \sin^3\Psi}{A^2(\Psi)} e^{-j\Gamma R \cos\theta \cos\Psi} J_o(\Gamma R \sin\theta \sin\Psi)\, d\Psi d\Gamma. \tag{2.39}$$

Again it will be useful to apply the same change of variables used for E_{zs}.

$$\begin{aligned} z &= R\cos\theta & \rho &= R\sin\theta \\ \gamma &= \Gamma\cos\Psi & u &= \Gamma\sin\Psi \end{aligned} \tag{2.40}$$

Applying these changes, (2.37) becomes

$$I_{fs1} = \int_{u=0}^{\infty} \int_{\gamma=-\infty}^{\infty} \frac{u^3}{(\varepsilon u^2 + \varepsilon_z \gamma^2)^2} e^{-j\gamma z} J_o(\rho u)\, d\gamma du. \tag{2.41}$$

To do the γ integration we need to evaluate

$$J = \int_{-\infty}^{\infty} \frac{e^{-j\gamma z}}{(\varepsilon u^2 + \varepsilon_z \gamma^2)^2} d\gamma. \tag{2.42}$$

This integration can be done with the aid of the residue theorem. One can close the integration path in the lower-half complex γ plane and evaluate the residue at the second-order pole, $\gamma = -j\sqrt{\varepsilon/\varepsilon_z}\, u$, obtaining

$$J = \frac{\pi}{2\varepsilon\ \varepsilon_z u^2}\ e^{-\sqrt{\varepsilon/\varepsilon_z}\ zu}\left[z + \frac{1}{\sqrt{\varepsilon/\varepsilon_z}\ u}\right] \tag{2.43}$$

Equation (2.41) becomes

$$I_{fs1} = \frac{\pi}{2\varepsilon\ \varepsilon_z}\int_0^\infty \left(uz + \frac{1}{\sqrt{\varepsilon/\varepsilon_z}}\right) e^{-\sqrt{\varepsilon/\varepsilon_z}\ zu}\ J_o(\rho u)\ du \tag{2.44}$$

or

$$I_{fs1} = \frac{\pi}{2\varepsilon\ \varepsilon_z}\left[\frac{z}{-\sqrt{\varepsilon/\varepsilon_z}}\frac{\partial}{\partial z} + \frac{1}{\sqrt{\varepsilon/\varepsilon_z}}\right]\int_0^\infty e^{-\sqrt{\varepsilon/\varepsilon_z}\ zu}\ J_o(\rho u)\ du \tag{2.45}$$

by recognizing the integral as the derivative of a different function.

Applying the integration formula

$$\int_0^\infty e^{-au}\ J_o(\rho u)\ du = \frac{1}{\sqrt{\rho^2 + a^2}} \tag{2.46}$$

obtained from Dwight [4], (2.45) may be written

$$I_{fs1} = \frac{\pi}{2\varepsilon^2\sqrt{\varepsilon_z}}\left[-z\frac{\partial}{\partial z} + 1\right]\frac{1}{\sqrt{\varepsilon^{-1}\rho^2 + \varepsilon_z^{-1}z^2}}\ . \tag{2.47}$$

Performing the indicated differentiation, E_{zfs1} may be finally written as

$$E_{zfs1} = \frac{-j\eta k_o}{8\pi\sqrt{\varepsilon}}\ \frac{1}{(\varepsilon_z\rho^2 + \varepsilon z^2)^{1/2}}\left[1 + \frac{\varepsilon z^2}{\varepsilon_z\rho^2 + \varepsilon z^2}\right] \tag{2.48}$$

or

$$E_{zfs1} = \frac{-j\eta k_o}{8\pi}\cdot\frac{1}{R'}\cdot\left[1 + \frac{\varepsilon z^2}{\varepsilon_z\rho^2 + \varepsilon z^2}\right]. \tag{2.48a}$$

The integration for E_{zfs2} will be done similarly. Using the same change of variables,

$$I_{fs2} = \int_{u=0}^{\infty} \int_{\gamma=-\infty}^{\infty} \frac{\gamma^2 u^3}{(\varepsilon u^2 + \varepsilon_z \gamma^2)^2 (u^2+\gamma^2)} e^{-j\gamma z} J_o(\rho u)\, d\gamma du. \quad (2.49)$$

Again the γ integration is done first

$$J = \int_{-\infty}^{\infty} \frac{\gamma^2 e^{-j\gamma z} d\gamma}{(\varepsilon u^2 + \varepsilon_z \gamma^2)^2 (u^2 + \gamma^2)}. \quad (2.50)$$

This integration can be performed with the aid of the residue theorem. Note in this case that there will be a pole at $\gamma = -u$ that did not occur for E_{zfs1}. One obtains the following equation

$$J = \frac{-\pi}{\varepsilon_z(\varepsilon_z - \varepsilon)u^3} \left\{ \frac{\varepsilon_z e^{-uz}}{\varepsilon_z - \varepsilon} + e^{-\sqrt{\varepsilon/\varepsilon_z}\, uz} \left[- \frac{\varepsilon_z + \varepsilon}{2\sqrt{\varepsilon/\varepsilon_z}(\varepsilon_z - \varepsilon)} + \frac{zu}{2} \right] \right\}. \quad (2.51)$$

The final integration of E_{zfs2} uses the exact methods as E_{zfs1} did. Differentiation with respect to z is moved outside the integral, the integration formula (2.46) is applied, and differentiation with respect to z is performed. After simplification one obtains

$$E_{zfs2} = \frac{j\eta k_o}{4\pi} \frac{\varepsilon'^2}{(\varepsilon_z - \varepsilon)} \left\{ \frac{1}{(\varepsilon_z - \varepsilon)} \frac{1}{\sqrt{z^2 + \rho^2}} - \frac{1}{2\sqrt{\varepsilon}} \frac{1}{\sqrt{\varepsilon_z \rho^2 + \varepsilon z^2}} \right. \quad (2.52)$$
$$\left. \cdot \left[\frac{\varepsilon_z + \varepsilon}{\varepsilon_z - \varepsilon} - \frac{\varepsilon z^2}{\varepsilon_z \rho^2 + \varepsilon z^2} \right] \right\}$$

or

$$E_{zfs2} = \frac{j\eta k_o}{4\pi} \frac{\varepsilon'^2}{(\varepsilon_z - \varepsilon)} \left\{ \frac{1}{(\varepsilon_z - \varepsilon)} \frac{1}{\sqrt{z^2 + \rho^2}} - \frac{1}{2R'} \left[\frac{\varepsilon_z + \varepsilon}{\varepsilon_z - \varepsilon} - \frac{\varepsilon z^2}{\varepsilon_z \rho^2 + \varepsilon z^2} \right] \right\}. \quad (2.52a)$$

2.5 Integrating E_{zf}

Equation (2.21), which defines E_{zf}, can be written

$$E_{zf} = j\eta k_o^3 \left(\frac{1}{2\pi}\right)^2 P(R, \theta) \tag{2.53}$$

$$P(R, \theta) = \int_0^{\pi} \int_0^{\infty} \frac{N(\Gamma, \Psi) e^{-j\Gamma R \cos\theta \cos\Psi}}{(\Gamma^2 - n_1^2 k_o^2)(\Gamma^2 - n_2^2 k_o^2)} J_o(\Gamma R \sin\theta \sin\Psi) \cdot \sin^3\Psi \, d\Gamma d\Psi \tag{2.54}$$

$$N(\Gamma, \Psi) = \Gamma^2[\varepsilon(\varepsilon^2 - \varepsilon'^2) - (n_1^2 + n_2^2)(\varepsilon^2 + \varepsilon'^2 \cos^2\Psi)] + n_1^2 n_2^2 (\varepsilon^2 + \varepsilon'^2 \cos^2\Psi) k_o^2 . \tag{2.55}$$

Note that the integrand of (2.54) is even in Ψ. Therefore, the limits of integration can be changed

$$P(R, \theta) = \int_0^{\pi/2} \int_{-\infty}^{\infty} \frac{N(\Gamma, \Psi) \sin^3\Psi e^{-j\Gamma Rp} J_o(\Gamma Rq)}{A^2(\Psi)(\Gamma^2 - n_1^2 k_o^2)(\Gamma^2 - n_2^2 k_o^2)} d\Gamma d\Psi \tag{2.56}$$

where we have also substituted

$$\begin{aligned} p &= \cos\theta \cos\Psi \\ q &= \sin\theta \sin\Psi \end{aligned} . \tag{2.57}$$

The Bessel function can be changed to a more tractable form by using the integral definition

$$J_o(\Gamma Rq) = \frac{1}{\pi} \int_0^{\pi/2} \left[e^{-j\Gamma Rq \cos\alpha} + e^{j\Gamma Rq \cos\alpha} \right] d\alpha. \tag{2.58}$$

Making this substitution and changing the order of integrations, we can organize $P(R, \theta)$ as

$$P(R, \theta) = \frac{1}{\pi} \int_0^{\pi/2} \int_0^{\pi/2} (I_1 + I_2) \frac{\sin^3 \Psi}{A^2(\Psi)} \, d\alpha d\Psi \tag{2.59}$$

where

$$I_1 = \int_{-\infty}^{\infty} \frac{N(\Gamma, \Psi) \, e^{-j\Gamma R(p + q \cos \alpha)}}{(\Gamma^2 - n_1^2 k_o^2)(\Gamma^2 - n_2^2 k_o^2)} \, d\Gamma \tag{2.60}$$

$$I_2 = \int_{-\infty}^{\infty} \frac{N(\Gamma, \Psi) \, e^{-j\Gamma R(p - q \cos \alpha)}}{(\Gamma^2 - n_1^2 k_o^2)(\Gamma^2 - n_2^2 k_o^2)} \, d\Gamma. \tag{2.61}$$

The next step is obviously integration by the residue method. However, one must take care to consider the signs of $(p + q \cos \alpha)$ and $(p - q \cos \alpha)$ for various ranges of Ψ and θ. Also one must remember that the square roots of n_1^2 and n_2^2 must be taken so that n_1 and n_2 have negative imaginary parts to satisfy the radiation condition.

For the range of the angles permitted by (2.59) for I_1, it can easily be seen $p + q \cos \alpha \geq 0$. Therefore, the integration path can be closed in the lower-half Γ plane to obtain

$$I_1 = \frac{-2\pi j}{k_o^3} \left[\frac{N(n_1 k_o, \Psi) \, e^{-jn_1 k_o R(p + q \cos \alpha)}}{2n_1(n_1^2 - n_2^2)} + \frac{N(n_2 k_o, \Psi) \, e^{-jn_2 k_o R(p + q \cos \alpha)}}{-2n_2(n_1^2 - n_2^2)} \right]. \tag{2.62}$$

For I_2, the sign of $(p - q \cos \alpha)$ depends on the exact range of θ, Ψ, and α. Recalling (2.57)

$$\begin{aligned} p &= \cos \theta \cos \Psi \\ q &= \sin \theta \sin \Psi, \end{aligned} \tag{2.57}$$

one can see

$p - q \cos\alpha \geq 0$ whenever either $0 \leq \Psi \leq \pi/2 - \theta$ and $0 \leq \alpha \leq \pi/2$ or whenever

$$\pi/2 - \theta \leq \Psi \leq \pi/2, \text{ and } \cos^{-1}\frac{p}{q} \leq \alpha \leq \pi/2. \tag{2.63}$$

In this case the integration path can also be closed in the lower-half Γ plane to obtain

$$I_2 = \frac{-2\pi j}{k_o^3}\left[\frac{N(n_1 k_o, \Psi)\, e^{-jn_1 k_o R(p - q\cos\alpha)}}{2n_1(n_1^2 - n_2^2)} + \frac{N(n_1 k_o, \Psi)\, e^{-jn_2 k_o R(p - q\cos\alpha)}}{-2n_2(n_1^2 - n_2^2)}\right]. \tag{2.64}$$

However,

$$p - q\cos\alpha \leq 0 \text{ for } \frac{\pi}{2} - \theta \leq \Psi \leq \frac{\pi}{2} \text{ and } 0 \leq \alpha \leq \cos^{-1}\frac{p}{q}. \tag{2.65}$$

Then, the integration path must be taken in the upper half of the complex-Γ plane to obtain

$$I_2 = \frac{2\pi j}{k_o^3}\left[\frac{N(-n_1 k_o, \Psi)\, e^{jn_1 k_o R(p - q\cos\alpha)}}{-2n_1(n_1^2 - n_2^2)} + \frac{N(-n_2 k_o, \Psi)\, e^{jn_2 k_o R(p - q\cos\alpha)}}{2n_2(n_1^2 - n_2^2)}\right]. \tag{2.66}$$

Gathering the results of (2.62), (2.64), and (2.66) and carefully noting over which range each is valid, we can rewrite (2.59). Note that N is an even function of its first argument, and that the second term of I_1 and I_2 is the first term with all n_1's and n_2's interchanged.

$$P(R, \theta) = R_{n1}(R, \theta) + P_{n2}(R, \theta) \tag{2.67}$$

$$P_{n2}(R, \theta) = P_{n1}(R, \theta) \text{ with } n_1 \text{ and } n_2 \text{ interchanged}$$

$$P_{n1}(R, \theta) = \frac{-j}{k_o^3}\int_0^{\pi/2}\int_0^{\pi/2} \frac{N(n_1 k_o, \Psi)\, e^{-jn_1 k_o R(p + q\cos\alpha)}}{n_1(n_1^2 - n_2^2)} \frac{\sin^3\Psi}{A^2(\Psi)}\, d\alpha d\Psi$$

$$-\frac{j}{k_o^3}\int_0^{\pi/2-\theta}\int_0^{\pi/2}\frac{N(n_1k_o,\Psi)\,e^{-jn_1k_oR(p-q\cos\alpha)}}{n_1(n_1^2-n_2^2)}\frac{\sin^3\Psi}{A^2(\Psi)}\,d\alpha d\Psi$$

$$-\frac{j}{k_o^3}\int_{\pi/2-\theta}^{\pi/2}\int_{\cos^{-1}p/q}^{\pi/2}\frac{N(n_1k_o,\Psi)\,e^{-jn_1k_oR(p-q\cos\alpha)}}{n_1(n_1^2-n_2^2)}\frac{\sin^3\Psi}{A^2(\Psi)}\,d\alpha d\Psi$$

$$-\frac{j}{k_o^3}\int_{\pi/2-\theta}^{\pi/2}\int_0^{\cos^{-1}p/q}\frac{N(n_1k_o,\Psi)\,e^{+jn_1k_oR(p-q\cos\alpha)}}{n_1(n_1^2-n_2^2)}\frac{\sin^3\Psi}{A^2(\Psi)}\,d\alpha d\Psi. \tag{2.68}$$

Note that the first integral's range can be broken into the ranges of the last three integrals. One can then distribute the integrand of the first integral to the last three. Recognizing the exponential form of the cosine function one finds

$$P_{n1}(R,\theta)=\int_0^{\pi/2-\theta}\int_0^{\pi/2}H(n_1,n_2,\Psi)\,e^{-jn_1k_oRp}\cos(n_1k_oRq\cos\alpha)\,d\alpha d\Psi$$

$$+\int_{\pi/2-\theta}^{\pi/2}\int_{\cos^{-1}p/q}^{\pi/2}H(n_1,n_2,\Psi)\,e^{-jn_1k_oRp}\cos(n_1k_oRq\cos\alpha)\,d\alpha d\Psi$$

$$+\int_{\pi/2-\theta}^{\pi/2}\int_0^{\cos^{-1}p/q}H(n_1,n_2,\Psi)\,e^{-jn_1k_oRq\cos\alpha}\cos(n_1k_oRp)\,d\alpha d\Psi \tag{2.69}$$

where we have let

$$H(n_1, n_2, \Psi) = \frac{-2j}{k_o^3} \frac{N(n_1 k_o, \Psi) \sin^3\Psi}{A^2(\Psi)\, n_1 (n_1^2 - n_2^2)} . \qquad (2.70)$$

A little algebra simplifies (2.70) to

$$H(n_1, n_2, \Psi) = \frac{-2j}{k_o} \frac{n_1[\varepsilon(\varepsilon^2 - \varepsilon'^2) - n_1^2(\varepsilon^2 + \varepsilon'^2 \cos^2\Psi)]\sin^3\Psi}{A^2(\Psi)(n_1^2 - n_2^2)} . \qquad (2.70a)$$

Now if we formally add and subtract the term

$$\int_{\pi/2-\theta}^{\pi/2} \int_{0}^{\cos^{-1} p/q} H(n_1, n_2, \Psi)\, e^{-jn_1 k_o R p} \cos(n_1 k_o R q \cos\alpha)\, d\alpha d\Psi$$

from $P_{n1}(R, \theta)$, it completes the range of one integral so that we can use the identity [5]

$$J_o(n_1 k_o R q) = \frac{2}{\pi} \int_0^{\pi/2} \cos(n_1 k_o R q \cos\alpha)\, d\alpha. \qquad (2.71)$$

Using these two manipulations, $P_{n1}(R, \theta)$ further simplifies to

$$P_{n1}(R, \theta) = \frac{\pi}{2} \int_0^{\pi/2} H(n_1, n_2, \Psi)\, e^{-jn_1 k_o R p} J_o(n_1 k_o R q)\, d\Psi$$

$$+ \int_{\pi/2-\theta}^{\pi/2} \int_0^{\cos^{-1} p/q} H(n_1, n_2, \Psi)[e^{-jn_1 k_o R q \cos\alpha} \cos(n_1 k_o R p) - e^{-jn_1 k_o R p}$$

$$\cdot \cos(n_1 k_o R q \cos\alpha)]\, d\alpha d\Psi. \qquad (2.72)$$

Simply expanding exponentials

$$P_{n1}(R, \theta) = \frac{\pi}{2} \int_0^{\pi/2} H(n_1, n_2, \Psi)\, e^{-jn_1 k_o R p} J_o(n_1 k_o R q)\, d\Psi$$

$$+ j \int_{\pi/2-\theta}^{\pi/2} \int_0^{\cos^{-1} p/q} H(n_1, n_2, \Psi) \sin n_1 k_o R(p - q\cos\alpha)\, d\alpha d\Psi. \qquad (2.73)$$

At this point it appears that no more exact simplifications are possible. It will be necessary then to make judicious approximations to put $P_{n1}(R, \theta)$ into a suitable form for calculation. The approximations will be easier to justify in cylindrical coordinates where

$$z = R \cos \theta$$
$$\rho = R \sin \theta. \tag{2.74}$$

Recall that z is to be interpreted as the distance along the antenna from the dipole source and ρ will be a, the radius of the antenna, which is assumed to be small compared to the length.

First, note that the sine term in the second integral of (2.73) is

$$\sin n_1 k_o [z \cos \Psi - a \sin \Psi \cos \alpha] = \sin (n_1 k_o z \cos \Psi) \cdot \cos (n_1 k_o a \sin \Psi \cos \alpha) - \cos (n_1 k_o z \cos \Psi) \sin (n_1 k_o a \sin \Psi \cos \alpha). \tag{2.75}$$

For small a we make a first-order approximation of (2.75) by

$$\sin (n_1 k_o z \cos \Psi) - n_1 k_o a \sin \Psi \cos \alpha \cos (n_1 k_o z \cos \Psi), \tag{2.76}$$

Now we can perform the indicated α integration in (2.73) on this simplified term (2.76) to get

$$\sin (n_1 k_o z \cos \Psi) \cos^{-1} \frac{z \cos \Psi}{a \sin \Psi} - n_1 k_o a \sin \Psi \cos (n_1 k_o z \cos \Psi) \sin \alpha \tag{2.77}$$

where

$$\sin \alpha = \sqrt{1 - \left[\frac{z \cos \Psi}{a \sin \Psi}\right]^2}.$$

We shall also make an approximation for the Bessel function in (2.73)

$$J_o(n_1 k_o R q) = J_o(n_1 k_o a \sin \Psi) \simeq 1 \tag{2.78}$$

for small a. Finally, we can write

$$P_{n1}(R, \theta) = \frac{\pi}{2} \int_0^{\pi/2} H(n_1, n_2, \Psi)\, e^{-jn_1 k_o z \cos \Psi}\, d\Psi$$

$$+ j \int_{\pi/2-\theta}^{\pi/2} H(n_1, n_2, \Psi) \left[\sin(n_1 k_o z) \cos \Psi \cos^{-1} \frac{z \cos \Psi}{a \sin \Psi} \right.$$

$$\left. - n_1 k_o a \sin \Psi \cos(n_1 k_o z \cos \Psi) \sqrt{1 - \left(\frac{z \cos \Psi}{a \sin \Psi} \right)^2} \right] d\Psi \qquad (2.79)$$

where

$$\theta = \tan^{-1} \frac{a}{z}.$$

2.6 Final Field Expressions for Infinitesimal Source

At last all the fields from an infinitesimal source have been found. They are repeated here for references purposes.

$$E_z = E_{zs} + E_{zfs1} + E_{zfs2} + E_{zf} \qquad (2.80)$$

$$E_{zs} = \frac{-j\eta\epsilon^2}{4\pi k_o \epsilon_z} \cdot \frac{1}{R'^3} \cdot \left[\frac{2\epsilon z^2 - \epsilon_z \rho^2}{\epsilon z^2 + \epsilon_z \rho^2} \right] \qquad (2.81)$$

$$E_{zfs1} = \frac{-j\eta k_o}{8\pi} \cdot \frac{1}{R'} \cdot \left[1 + \frac{\epsilon z^2}{\epsilon z^2 + \epsilon_z \rho^2} \right] \qquad (2.82)$$

$$E_{zfs2} = \frac{j\eta k_o}{4\pi} \frac{\epsilon'^2}{\epsilon_z - \epsilon} \left\{ \frac{1}{\epsilon_z - \epsilon} \frac{1}{\sqrt{z^2 + \rho^2}} - \frac{1}{2R'} \left[\frac{\epsilon_z + \epsilon}{\epsilon_z - \epsilon} - \frac{\epsilon z^2}{\epsilon z^2 + \epsilon_z \rho^2} \right] \right\} \qquad (2.83)$$

$$R' = \sqrt{\epsilon} \sqrt{\epsilon z^2 + \epsilon_z \rho^2} \qquad (2.83a)$$

$$E_{zf} = j\eta k_o \left(\frac{k_o}{2\pi}\right)^2 [P_{n1}(z, \rho) + P_{n2}(z, \rho)] \qquad (2.84)$$

$$P_{n1}(z, \rho) = \frac{\pi}{2} \int_0^{\pi/2} H(n_1, n_2, \Psi)\, e^{-jn_1 k_o z \cos \Psi}\, d\Psi$$

$$+ j \int_{\pi/2-\theta}^{\pi/2} H(n_1, n_2, \Psi) \left[\sin(n_1 k_o z \cos \Psi) \cos^{-1} \frac{z \cos \Psi}{a \sin \Psi}\right.$$

$$\left. - n_1 k_o a \sin \Psi \cos(n_1 k_o z \cos \Psi) \sqrt{1 - \left(\frac{z \cos \Psi}{a \sin \Psi}\right)^2}\right] d\Psi \qquad (2.85)$$

where

$$\theta = \tan^{-1} \frac{a}{z}$$

$$H(n_1, n_2, \Psi) = \frac{-2j}{k_o} n_1 \frac{[\varepsilon(\varepsilon^2 - \varepsilon'^2) - n_1^2(\varepsilon^2 + \varepsilon'^2 \cos^2 \Psi)] \sin^3 \Psi}{A^2(\Psi)(n_1^2 - n_2^2)} \qquad (2.85a)$$

$$n_1^2, n_2^2 = \frac{B(\Psi) \pm \sqrt{B^2(\Psi) - 4A(\Psi)C(\Psi)}}{2A(\Psi)} \quad ; \quad \mathrm{Im}(n_1) < 0, \ \mathrm{Im}(n_2) < 0 \qquad (2.86)$$

$$A(\Psi) = \varepsilon \sin^2 \Psi + \varepsilon_z \cos^2 \Psi$$

$$B(\Psi) = \varepsilon\varepsilon_z(1 + \cos^2 \Psi) + (\varepsilon^2 - \varepsilon'^2) \sin^2 \Psi \qquad (2.87)$$

$$C(\Psi) = (\varepsilon^2 - \varepsilon'^2)\, \varepsilon_z \qquad (2.88)$$

$P_{n2} = P_{n1}$ with all n_1's and n_2's interchanged.

CHAPTER III. APPLICATION OF METHOD OF MOMENTS

In the last section we derived an expression for the electric field produced by an infinitesimal source. It can easily be seen that the current distribution on the antenna, i(z), must satisfy the integral equation

$$\int_0^{\ell} i(z')\, K(z - z')\, dz' = e(z) \tag{3.1}$$

where e(z) is $\begin{cases} E \text{ applied at antenna feed,} \\ 0 \text{ everywhere else} \end{cases}$

and where ℓ is the length of the antenna, and $K(z - z') = E_z(z - z')$ is the Green's function evaluated on the surface of the antenna. Thus (3.1) basically specifies that the tangential E field on the surface of the antenna must be zero.

The general theory of the method of moments will be presented, following the formulation by Harrington [6]. Then it will be shown how this method can be applied to this problem. First define the inner product of two functions on some interval I as

$$\langle f(z), g(z) \rangle = \int f(z)\, g(z)\, dz. \tag{3.2}$$

Now consider solving the inhomogeneous equation

$$L(f) = g \tag{3.3}$$

where f and g are functions defined on the common interval I, L is a linear operator, g is known, and f is unknown.

Suppose f is approximated as a sum of n known functions weighted by n unknown coefficients α_n.

$$f = \sum_{j=1}^{n} \alpha_j f_j . \tag{3.4}$$

The f_j functions are called expansion functions. Now by substituting (3.4) into (3.3) and using the linearity of L, the equation becomes

$$\sum_{j=1}^{n} \alpha_j L(f_j) = g. \tag{3.5}$$

Now define a set of n weighting functions or testing functions, w_i, i = 1, n. By taking the inner product of both sides of (3.5) with respect to each testing function, the equation becomes

$$\sum_{j=1}^{n} \alpha_j < w_i, Lf_j > = < w_i, g>, \quad i = 1, 2, \cdots n. \tag{3.6}$$

This can be written in matrix form as

$$[\ell_{ij}][\alpha_j] = [g_i] \tag{3.7}$$

where

$$[\ell_{ij}] = \begin{bmatrix} < w_1, Lf_1 > & < w_1, Lf_2 > & \cdots \\ < w_2, Lf_1 > & < w_2, Lf_2 > & \cdots \\ \cdots & \cdots & \cdots \end{bmatrix} \tag{3.8}$$

$$[\alpha_j] = \begin{bmatrix} \alpha_1 \\ \alpha_2 \\ \cdot \\ \cdot \\ \cdot \\ \alpha_n \end{bmatrix} \qquad [g_i] = \begin{bmatrix} g_1 \\ g_2 \\ \cdot \\ \cdot \\ \cdot \\ g_n \end{bmatrix} = \begin{bmatrix} < w_1, g > \\ < w_2, g > \\ \cdot \\ \cdot \\ \cdot \\ < w_n, g > \end{bmatrix} . \tag{3.9}$$

Equation (3.7) can be solved for $[\alpha_j]$ simply by inversion, provided $[\ell_{ij}]$ is nonsingular

$$[\alpha_j] = [\ell_{ij}]^{-1}[g_i]. \tag{3.10}$$

Thus, f has been solved as a weighted sum of the expansion functions.

The method of moments, as it has thus been described, is very general. The particular choice of expansion and testing functions used for this problem will simplify the form of the solution considerably. Also, this choice affects the accuracy attainable for a given number of functions. Now we will show how to apply the method to this antenna problem by first identifying the functions and operators in (3.3). The unknown function f is i(z) defined on the interval [0, ℓ] representing the antenna. Likewise, the known function g is the tangential electric field e(z). The linear operator L is the integral operator

$$L(h) = \int_0^{\ell} h(z')\, E_z(z - z')\, dz' \tag{3.11}$$

or described in words, convolution with the Green's function along the antenna.

Next expansion functions must be devised for i(z). We will follow what is called the method of subsections, that is, expansion functions are chosen that are defined on only a subsection of the antenna interval. First, the antenna is divided into odd n number of segments, where each segment has length $\frac{2H}{n}$. Then, the expansion functions are defined as the pulse functions

$$p_i(z) = \begin{cases} 1 & \text{if } (i-1)\frac{2H}{n} \leq z \leq i\left(\frac{2H}{n}\right) \\ 0 & \text{otherwise} \end{cases} . \tag{3.12}$$

Now we can express i(z) as

$$i(z) = \sum_{i=1}^{n} i_i\, p_i(z). \tag{3.13}$$

Figure 2 shows how the use of pulse expansion functions replaces the actual current with a step approximation.

Now a set of testing functions must be chosen. The simplest choice utilizes the point-matching method. For this method, we choose w_i to be $\delta(z - m_i)$, where $\delta(z)$ is the Dirac delta function and m_i is the midpoint of the i^{th} antenna segment. Thus, by the sampling property of the δ function, the right-hand side of (3.6) is

$$< w_i, g > = g(m_i). \tag{3.14}$$

Therefore, for this problem $[g_i] = [e_i]$, where $[e_i]$ is the vector of tangential electric fields evaluated at the midpoint of each segment. Similarly, we can see that element ℓ_{ij} of (3.8) is the electric field at the midpoint of the i^{th} segment caused by the uniform current over the j^{th} segment.

Finally, the original integral equation (3.1) has been transformed into the following matrix equation

$$Z\, I = E \tag{3.15}$$

where $Z = [z_{ij}]$; z_{ij} is the electric field produced by the uniform current over the j^{th} segment evaluated at the midpoint of the i^{th} segment.

$$I = \begin{bmatrix} i_1 \\ i_2 \\ \cdot \\ \cdot \\ \cdot \\ i_n \end{bmatrix} \quad i_k \text{ is the current over } k^{th} \text{ segment} \qquad E = \begin{bmatrix} 0 \\ 0 \\ 0 \\ E \text{ applied} \\ 0 \\ 0 \\ 0 \end{bmatrix} \quad \text{tangential electric field at midpoint of } k^{th} \text{ segment}$$

The solution is obviously

$$I = Z^{-1} E = YE. \tag{3.16}$$

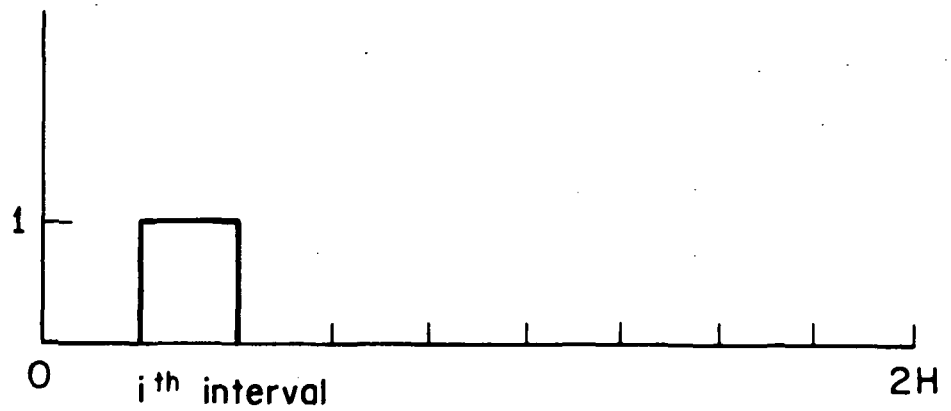

PULSE FUNCTION $p_i(z)$

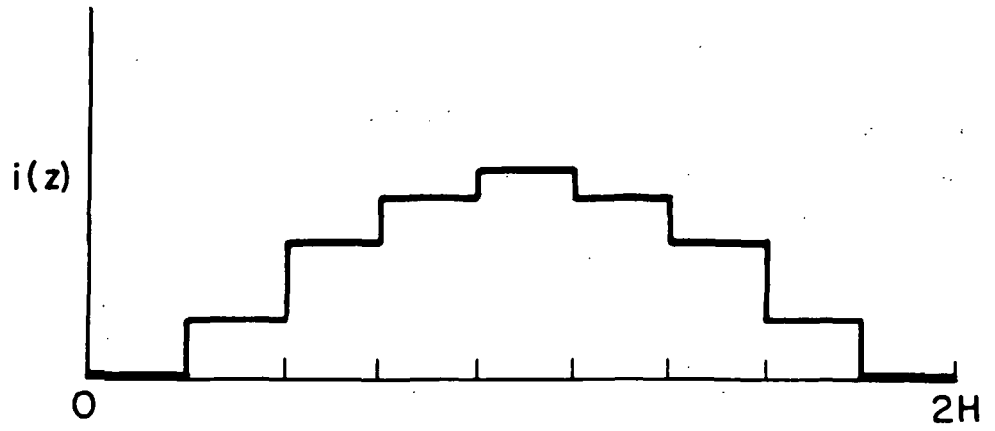

PULSE FUNCTION EXPANSION FOR i(z)

Figure 2. Use of Pulse Expansion Functions

Suppose the feed is at the k^{th} segment. Then the impedance of the antenna is simply $\frac{v_k}{i_k}$ where v_k is the voltage over the gap. In this report the feed is always at the center of the antenna.

Note some very important properties of the matrix Z. First, there are only n unique elements. Segments the same distance apart have the same effect on each other. Thus $z_{ij} = z_{i+k,j+k}$. Also, by symmetry $z_{ij} = z_{ji}$. Therefore we can write Z as

$$Z = \begin{bmatrix} z_1 & z_2 & z_3 & \cdot & \cdot & \cdot & z_n \\ z_2 & z_1 & z_2 & & & & \\ z_3 & z_2 & z_1 & & & & \\ \cdot & & & \cdot & & & \\ \cdot & & & & \cdot & & \\ \cdot & & & & & \cdot & z_2 \\ z_n & & & & & z_2 & z_1 \end{bmatrix} \quad (3.17)$$

The matrix Z is a complex symmetric matrix. Unfortunately, most of the useful properties of real symmetric matrices or complex Hermitian matrices do not apply to complex symmetric matrices. The element z_1 is called the self-element since it is the field at the midpoint of a segment carrying a uniform current. Since the fields decrease strongly with distance, it will be shown that Z is strongly diagonal.

The Z matrix has been discussed somewhat generally. Next, we will discuss the method for calculating the elements from the Green's function derived in the last section. There are three different sets of

expressions based on three different models for the distribution of current over one segment. The basic model used assumes that the current over one segment is uniformly distributed over the axis line; this current distribution will be called the current filament model. Since the field is evaluated at the radius, it remains finite.

Recalling that the length of one segment is $2\Delta\ell$, we can write the field caused by the current filament as the superposition of fields caused by infinitesimal sources distributed along the filament. Thus,

$$E_{z\ \text{filament}}(z, a) = \frac{1}{2\Delta\ell} \int_{-\Delta\ell}^{\Delta\ell} E_z(z - z', a)\, dz'. \qquad (3.18)$$

The factor of $1/2\Delta\ell$ is included to make the effective current over the segment equal for the two models. This integration was done on each of the four component fields of E_z. For E_{zs}, E_{zfs1}, and E_{zfs2}, one must perform integrals of the form

$$I = \int_{-\Delta\ell}^{\Delta\ell} \frac{(z - z')^n}{[(z - z')^2 + a^2]^m}\, dz' \qquad (3.19)$$

where n is 0 or 2 and m is 1/2, 3/2, or 5/2. These integrals can be found in common integral tables. Therefore, the integrated forms of E_{zs}, E_{zfs1}, and E_{zfs2} will be simply presented later.

Integrating E_{zf}, the component of the Green's function E_z, which cannot be written in closed form, requires more explanation. Recall that E_{zf} is given by (2.84)

$$E_{zf} = j\eta k_o \left(\frac{k_o}{2\pi}\right)^2 [P_{n1}(z, \rho) + P_{n2}(z, \rho)]. \qquad (2.84)$$

The first term can be written as

$$P_{n1} = I_{zfa} + I_{zfb} \tag{3.20}$$

where

$$I_{zfa} = \frac{\pi}{2} \int_0^{\pi/2} H(n_1, n_2, \Psi)\, e^{-jn_1 k_o z \cos \Psi}\, d\Psi \tag{3.21}$$

$$I_{zfb} = j \int_{\pi/2-\theta}^{\pi/2} H(n_1, n_2, \Psi) \left[\sin(n_1 k_o z \cos \Psi) \cos^{-1}\left(\frac{z \cos \Psi}{a \sin \Psi}\right) - n_1 k_o a \sin \Psi \cos(n_1 k_o z \cos \Psi) \sqrt{1 - \left(\frac{z \cos \Psi}{a \sin \Psi}\right)^2} \right] d\Psi \tag{3.22}$$

where

$$\theta = \tan^{-1} \frac{a}{z}.$$

Remember n_1, n_2 and H are functions of Ψ.

We will make the approximation that I_{zfb} can be neglected. To justify this, first note that the integration width for the self-element where $z = 0$ is $\theta = \frac{\pi}{2}$. For the first segment away from the source element, $z = 2\Delta\ell$, and since only thin wires are being treated, $\frac{a}{z}$ is small. Therefore for all elements, except the self-element, $\theta \simeq \frac{a}{z}$. We can now make small angle approximations in (3.22) and perform the integration to get

$$I_{zfb} \simeq -j\, H(n_1, n_2, \tfrac{\pi}{2})\, \frac{3\pi}{8}\, n_1\, k_o\, \frac{a^2}{z}, \qquad z \geq 2\Delta\ell. \tag{3.23}$$

Because of the $\frac{a^2}{z}$ term, I_{zfb} should be small compared to I_{zfa}. For $z = 0$, Equation (3.22) simplifies to

$$I_{zfb} = j \int_0^{\pi/2} H(n_1, n_2, \Psi)\, n_1\, k_o a \sin \Psi\, d\Psi. \tag{3.24}$$

Direct numerical integration of (3.21), (3.22), and (3.24) indicates that I_{zfb} may be neglected for all terms including the self-element.

Moreover, one should note that the singular field terms are orders of magnitude larger than E_{zf} for all but the farthest segments; therefore, E_{zf} need not have an extremely small relative error.

Now, when I_{zfb} is neglected, E_{zf} can be integrated over one segment, according to (3.18). Note that z occurs only in the exponential $e^{-jn_1k_oz\cos\Psi}$. Therefore, one obtains the integrated form of E_{zf} by integrating the exponential. One can easily verify that

$$\frac{1}{2\Delta\ell}\int_{-\Delta\ell}^{\Delta\ell} e^{-jn_1k_o(z-z')\cos\Psi}\,dz' = e^{-jn_1k_oz\cos\Psi}\left[\frac{\sin(n_1k_o\cos\Psi\,\Delta\ell)}{n_1k_o\cos\Psi\,\Delta\ell}\right]. \tag{3.25}$$

One does the exact same integration for the exponential containing n_2. The integrated form of E_{zf} is then only E_{zf} with the exponentials replaced by the right-hand side of (3.25).

We will summarize the fields produced by a current filament mode. To avoid proliferation of variable names, the integrated form has the same name as the corresponding term of the Green's function. We have substituted the antenna radius a for ρ.

$$E_{z\ \text{filament model}} = E_{zs} + E_{zfs1} + E_{zfs2} + E_{zf} \tag{3.26}$$

$$E_{zs} = \frac{j\eta}{8\pi k_o\epsilon\Delta\ell}\left[\frac{z+\Delta\ell}{[(z+\Delta\ell)^2+a'^2]^{3/2}} - \frac{z-\Delta\ell}{[(z-\Delta\ell)^2+a'^2]^{3/2}}\right] \tag{3.27}$$

where $a'^2 = \frac{\epsilon_z}{\epsilon}a^2$

$$E_{zfs1} = \frac{-jk_o\eta}{8\pi(2\Delta\ell)}\left\{2\,\ell n\,\frac{z+\Delta\ell+\sqrt{(z+\Delta\ell)^2+a'^2}}{z-\Delta\ell+\sqrt{(z-\Delta\ell)^2+a'^2}} - \frac{z+\Delta\ell}{\sqrt{(z+\Delta\ell)^2+a'^2}} + \frac{z-\Delta\ell}{\sqrt{(z-\Delta\ell)^2+a'^2}}\right\} \tag{3.28}$$

$$E_{zfs2} = \frac{jk_o\eta}{4\pi} \frac{\varepsilon'^2}{(\varepsilon_z - \varepsilon)} \frac{1}{2\Delta\ell} \left\{ \frac{1}{\varepsilon_z - \varepsilon} \ell n \frac{z + \Delta\ell + \sqrt{(z + \Delta\ell)^2 + a^2}}{z - \Delta\ell + \sqrt{(z - \Delta\ell)^2 + a^2}} \right.$$

$$- \frac{1}{\varepsilon_z - \varepsilon} \ell n \frac{z + \Delta\ell + \sqrt{(z + \Delta\ell)^2 + a'^2}}{z - \Delta\ell + \sqrt{(z - \Delta\ell)^2 + a'^2}}$$

$$\left. - \frac{1}{2\varepsilon} \left(\frac{z + \Delta\ell}{\sqrt{(z + \Delta\ell)^2 + a'^2}} - \frac{z - \Delta\ell}{\sqrt{(z - \Delta\ell)^2 + a'^2}} \right) \right\} \qquad (3.29)$$

$$E_{zf} = j\eta k_o \left(\frac{k_o}{2\pi} \right)^2 (P_{n1} + P_{n2}) \qquad (3.30)$$

$$P_{n1} = \frac{\pi}{2} \int_0^{\pi/2} H(n_1, n_2, \Psi)\, e^{-jn_1 k_o z \cos\Psi} \cdot \frac{\sin(n_1 k_o \cos\Psi\, \Delta\ell)}{n_1 k_o \cos\Psi\, \Delta\ell}\, d\Psi \qquad (3.31)$$

$$H(n_1, n_2, \Psi) = -\frac{2j}{k_o} n_1 \frac{[\varepsilon(\varepsilon^2 - \varepsilon'^2) - n_1^2(\varepsilon^2 + \varepsilon'^2 \cos^2\Psi)] \sin^3\Psi}{A^2(\Psi)\,(n_1^2 - n_2^2)} \qquad (3.32)$$

$$n_1^2,\ n_2^2 = \frac{B(\Psi) \pm \sqrt{B^2(\Psi) - 4A(\Psi)\, C(\Psi)}}{2A(\Psi)} \quad ; \quad \mathrm{Im}(n_1) < 0, \quad \mathrm{Im}(n_2) < 0 \qquad (3.33)$$

$$A(\Psi) = \varepsilon \sin^2\Psi + \varepsilon_z \cos^2\Psi \qquad (3.34)$$

$$B(\Psi) = \varepsilon\varepsilon_z(1 + \cos^2\Psi) + (\varepsilon^2 - \varepsilon'^2) \sin^2\Psi$$

$$C(\Psi) = (\varepsilon^2 - \varepsilon'^2)\, \varepsilon_z$$

$$P_{n2} = P_{n1} \text{ with all } n_1\text{'s and } n_2\text{'s interchanged.} \qquad (3.35)$$

Equations (3.32) to (3.35) are the same as Equations (2.80) to (2.89) but are reproduced for reference.

It has been shown [7] that one obtains better answers if $\sqrt{2}\,a$ is used in the calculations as an effective radius in place of a. This correction compensates for the assumption that the current is on the axis instead of distributed on the surface.

One can note that many simplifications in the preceding formulas are possible and in many cases necessary for limiting cases of the general anisotropic plasma. For free space, the E_{zfs2} term has zeros in both the numerator and the denominator. One can clearly see that for plasma parameters X = 0, corresponding physically to free space with an applied magnetic field, and that for $Y^2 = 0$, corresponding physically to an isotropic plasma, there is no off-diagonal dielectric element ε' and, therefore, $E_{zfs2} = 0$. In the limiting case of free space, E_{zfs2} must be set equal to zero. One must also analytically treat removable singularities in the expressions for E_{zf}. For the isotropic case, the two indices of refraction n_1 and n_2 are equal. The expression for H can be rewritten to avoid an indeterminate form.

Next one can compare the fields produced by the current filament model to the fields produced by δ-source model. The δ-source model is physically unrealistic; however, it should give the same values as the filament model for observation points far from the segment with the current. Far from the source, numerical calculations show that for all field components one may use the δ-source model to avoid subtracting nearly equal terms present in the filament model expression. In general, no more than 21 segments were used and, therefore, the δ-source model was not needed for computation. One can note that the

E_{zf} term is nearly independent of distance. Therefore, one would not expect the fields due to the two models to be significantly different for any distance. Calculations verify this.

A third current distribution model was considered. One might object to the filament model as being unrealistic, especially for elements very close to the current segment. Therefore, we have examined a model for which the current is uniform on the surface of the segment. We call this model the cylindrical current model. This model can be obtained from the filament model by summing up the contribution of distributed current filaments placed along the surface of the current segment. When one integrates around the segment, one needs to replace the radius a with the radial distance $2a \sin \frac{\phi}{2}$. (See Figure 3.) Recall that E_z has the form $E_z(z, a)$. Therefore, we write

$$E_{z \text{ cylindrical}} = \frac{1}{2\pi} \int_0^{2\pi} E_{z \text{ filament}} \left(z, 2a \sin \frac{\phi}{2}\right) d\phi. \tag{3.36}$$

Since the cylindrical model is needed only in the very near region, and since in this region the E_{zs} term strongly dominates the other terms, this cylindrical integration is applied only to the E_{zs} term. Then substituting $E_{zs \text{ filament}}$ into Equation (3.36) one obtains

$$E_{zs \text{ cylindrical}} = \frac{1}{2\pi} \int_0^{2\pi} \frac{jn}{8\pi k_o \epsilon \Delta\ell} \cdot \left[\frac{z + \Delta\ell}{\left[(z + \Delta\ell)^2 + 4a'^2 \sin^2 \frac{\phi}{2}\right]^{3/2}} - \frac{z - \Delta\ell}{\left[(z - \Delta\ell)^2 + 4a'^2 \sin^2 \frac{\phi}{2}\right]^{3/2}} \right] d\phi \tag{3.37}$$

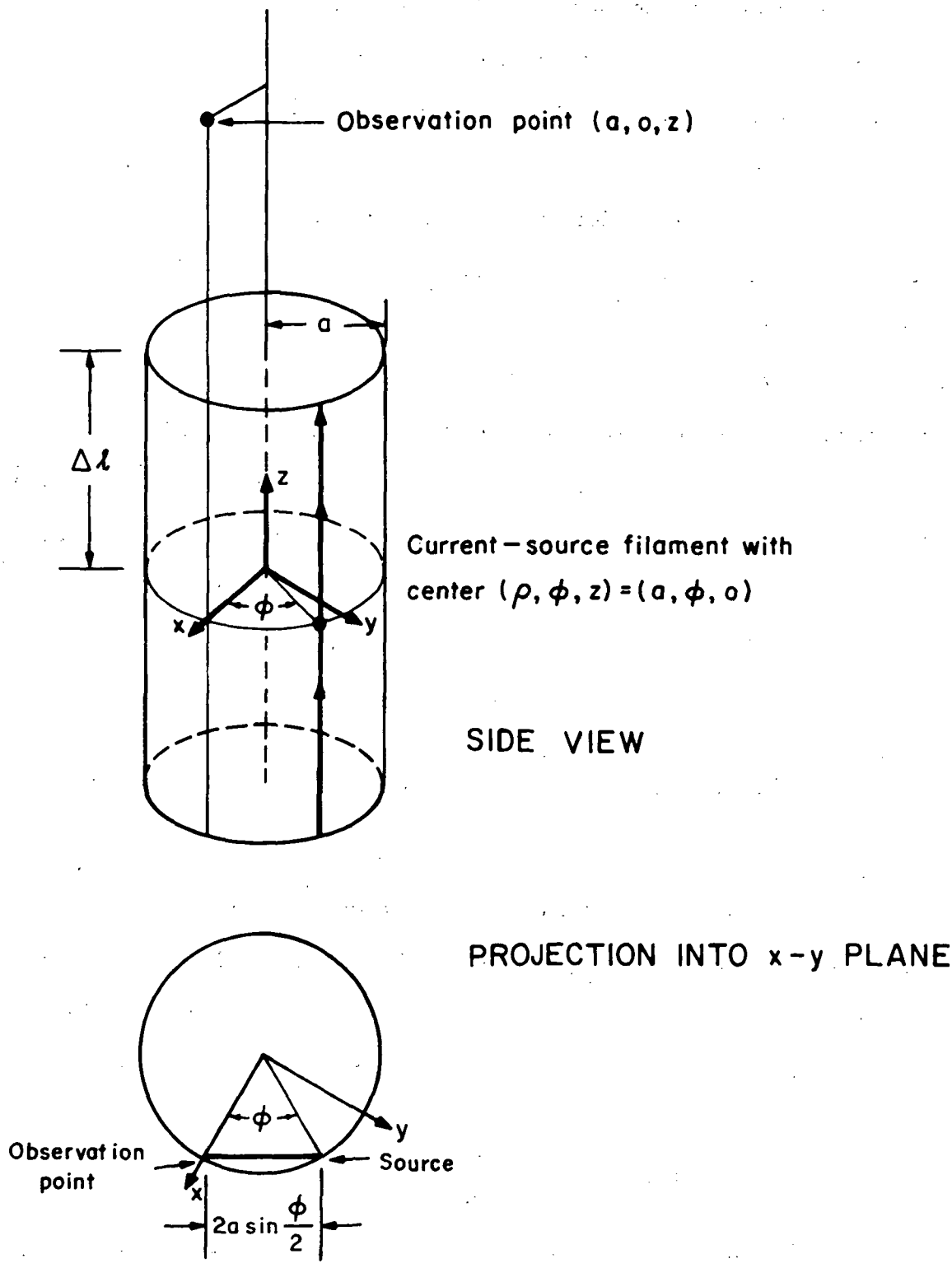

Figure 3. Cylindrical Model as Distributed Current Filaments on Surface of Segment

One can see that (3.37) essentially is an integral of the form

$$I = \frac{1}{2\pi} \int_0^{2\pi} \frac{d\phi}{[4a'^2 \sin^2 \frac{\phi}{2} + b^2]^{3/2}} \tag{3.38}$$

Making the change of variable

$$\theta = \phi + \pi \tag{3.39}$$

and simplifying yields

$$I = \frac{1}{4\pi a'^3} k^3 \int_0^{\pi/2} \frac{d\theta}{(1 - k^2 \sin^2\theta)^{3/2}} \tag{3.40}$$

where

$$k = \frac{2a'}{(b^2 + 4a'^2)^{1/2}} \quad \text{and} \quad a'^2 = \frac{\epsilon_z}{\epsilon} a^2. \tag{3.41}$$

Note how similar (3.40) is to the definition of an elliptic integral. Applying a clever transform from Gradshteyn and Ryzhik [8] allows us to write

$$I = \frac{1}{4\pi a'^3} \frac{k^3}{1 - k^2} E(k) \tag{3.42}$$

where E(k) is an elliptic integral of the second kind. Equation (3.42) can be applied to (3.37) to obtain

$$E_{zs\ \text{cylindrical}} = \frac{j\eta}{8\pi k_o \epsilon \Delta\ell} \left[\frac{z + \Delta\ell}{4\pi a'^3} \frac{k_+^3}{1 - k_+^2} E(k_+) - \frac{(z - \Delta\ell)}{4\pi a'^3} \frac{k_-^3}{1 - k_-^2} E(k_-) \right] \tag{3.43}$$

$$k_+ = \frac{2a'}{[(z + \Delta\ell)^2 + 4a'^2]^{1/2}}, \quad k_- = \frac{2a'}{[(z - \Delta\ell)^2 + 4a'^2]^{1/2}}.$$

Now one can compare the fields due to a current filament to the fields due to the equivalent current flowing on the cylindrical surface. Although one might expect much different values for the most singular

terms, the results were extremely close. Except near $z = \Delta\ell$, the fields generally agree to better than 1 per cent. See Table 1 for a comparison of the two models for various distances and plasma parameters.

One can note that the field for the cylindrical model is singular for $z = \Delta\ell$, and that it changes sign crossing this point. This can easily be understood from a quasi-static model. From this viewpoint, the current causes rings of charge to accumulate on the edges of the cylinder, and the electric field is the electrostatic field due to these two rings. Clearly for $z = \Delta\ell$, one is evaluating the field at the ring and it is singular there. The filament model remains finite at $z = \Delta\ell$ because for this model the charge is on the axis, an effective distance of a' from the point of observation.

After comparing the three current distribution models, we decided that the filament model was entirely adequate for E_{zfs1}, E_{zfs2}, and E_{zf}. For E_{zs} we use the cylindrical model although it is only slightly different from the filament model. Therefore, each element z_i of Z, as shown in (3.17), is computed as

$$z_i = E_z [(i - 1)\ 2\Delta\ell, a] \qquad (3.44)$$

where

$$E_z = E_z(z, a);$$

the cylindrical model of E_z is used for E_{zs} and the filament model is used for E_{zfs1}, E_{zfs2}, and E_{zf}.

There are still a few small matters to discuss before calculating I, the current vector. First, one may consider applying one volt to the feed obtaining the resulting electric field

TABLE 1.

COMPARISON OF ELECTRIC FIELDS DUE TO FILAMENT AND CYLINDRICAL CURRENT DISTRIBUTION MODELS

$H = 1, \quad a = 1/144., \quad \Delta\ell = \frac{1}{23} \quad k_o = .1, \quad z = m2\Delta\ell$

X Y^2 Z	segments m	E_{zs} cylindrical (z, a)		E_{zs} filament (z, $\sqrt{2}$ a)	
		REAL	IMAG	REAL	IMAG
0 0 . 0	0	0.0	$.3395\times10^{7}$	0.0	$.3388\times10^{7}$
	.43	0.0	$.2737\times10^{8}$	0.0	$.1418\times10^{8}$
	1	0.0	$-.1496\times10^{7}$	0.0	$-.1493\times10^{7}$
	2	0.0	$-.1283\times10^{6}$	0.0	$-.1283\times10^{6}$
	5	0.0	-7437.	0.0	-7437.
	10	0.0	-916.8	0.0	-916.8
.1 .1 .05	0	$-.2862\times10^{5}$	$.3814\times10^{7}$	$-.2835\times10^{5}$	$.3806\times10^{7}$
	.43	$-.2067\times10^{6}$	$.3059\times10^{8}$	$-.8602\times10^{5}$	$.1574\times10^{8}$
	1	$.1260\times10^{5}$	$-.1681\times10^{7}$	$.1246\times10^{5}$	$-.1677\times10^{7}$
	2	1094.	$-.1442\times10^{6}$	1093.	$-.1442\times10^{6}$
	5	63.54	-8362.	63.53	-8362.
	10	7.834	-1031.	7.834	-1031.

TABLE 1. (CONTINUED)

X	Y^2	Z	segments m	E_{zs} cylindrical (z,a)		E_{zs} filament (z, $\sqrt{2}$ a)	
				REAL	IMAG	REAL	IMAG
.9	.9	.05	0	$-.4836\times10^{6}$	$-.4101\times10^{6}$	$-.4838\times10^{6}$	$-.4099\times10^{6}$
			.43	$-.1258\times10^{8}$	$-.9702\times10^{7}$	$-.1283\times10^{8}$	$-.9433\times10^{7}$
			1	$.2150\times10^{6}$	$.1822\times10^{6}$	$.2150\times10^{6}$	$.1821\times10^{6}$
			2	$.1718\times10^{5}$	$.1459\times10^{5}$	$.1718\times10^{5}$	$.1459\times10^{5}$
			5	985.6	837.4	985.6	837.4
			10	121.4	103.1	121.4	103.1
.2	.25	.05	0	$-.2767\times10^{6}$	$-.2084\times10^{7}$	$-.2754\times10^{6}$	$-.2082\times10^{7}$
			.43	$-.2534\times10^{7}$	$-.2088\times10^{8}$	-1.440×10^{7}	$-.1382\times10^{8}$
			1	$.1223\times10^{6}$	$.9215\times10^{6}$	$.1216\times10^{6}$	$.9207\times10^{6}$
			2	$.1028\times10^{5}$	$.7692\times10^{5}$	$.1027\times10^{5}$	$.7692\times10^{5}$
			5	594.0	4441.	594.0	4441.
			10	73.20	574.2	73.20	547.2

TABLE 1. (CONTINUED)

X Y^2 Z	segments m	E_{zs} cylindrical (z, a)		E_{zs} filament (z, $\sqrt{2}$ a)	
		REAL	IMAG	REAL	IMAG
2. 2. .05	0	$-.1291\times10^{6}$	$.1250\times10^{7}$	$-.1312\times10^{6}$	$.1249\times10^{7}$
	.43	$-.1857\times10^{8}$	$.2765\times10^{7}$	$-.2355\times10^{9}$	$.8449\times10^{8}$
	1	$.5776\times10^{5}$	$-.5571\times10^{6}$	$.5877\times10^{5}$	$-.5568\times10^{6}$
	2	4361.	-4350×10^{5}	4372.	$-.4349\times10^{5}$
	5	248.4	-2488.	248.5	-2488.
	10	30.55	-306.2	30.56	-306.2
.5 2. .05	0	$-.1180\times10^{6}$	$.2381\times10^{6}$	$-.1180\times10^{6}$	$.2380\times10^{7}$
	.43	$-.1499\times10^{7}$	$.3021\times10^{8}$	$-.1208\times10^{7}$	$.243\times10^{8}$
	1	$.5231\times10^{5}$	$-.1055\times10^{7}$	$.5231\times10^{5}$	$-.1055\times10^{7}$
	2	4288.	$-.8647\times10^{5}$	4288.	$-.8647\times10^{5}$
	5	426.9	-4979.	246.9	-4979.
	10	30.41	-613.4	30.41	-613.4

$$E_{feed} = -\frac{V_{feed}}{d} = -\frac{V_{feed}}{2\Delta\ell} = -\frac{1}{2\Delta\ell}\ , \qquad (3.45)$$

since the gap distance d is $2\Delta\ell$. Second, note that $E_{z\ filament}$ gives the field due to a distributed source with the same effective current as the δ-source model. This δ source was one ampere at one point; when it is distributed, the current at any point is only $\frac{1}{2\Delta\ell}$ ampere. Therefore, one should multiply all elements of Z by $2\Delta\ell$ to get true fields. Equivalently, this last factor of $2\Delta\ell$ is factored from the Z matrix into the E vector. Therefore, considering both comments about the $2\Delta\ell$ factor, the vector E is computed as

$$E = [e_i] = \begin{cases} -\dfrac{1}{(2\Delta\ell)^2}\ , & i = \text{center element} \\ 0\ , & i \neq \text{center element} \end{cases} . \qquad (3.46)$$

One must also make slight corrections between effective and actual dimensions of the antenna. The use of pulse expansion functions assumes a finite current at the end of the antenna when the true current must be zero. To compensate for this, dummy segments have been added to each end. These segments are not used in calculations, but only make the length of the antenna for which the nonzero currents can exist shorter than the actual physical length 2H. Therefore, for segments one uses

$$2\Delta\ell = \frac{2H}{n+2} \qquad \text{instead of } 2\Delta\ell = \frac{2H}{n}\ .$$

The exact number of segments to add was partially determined empirically. Using one extra segment on each end results in a good, but not perfect, linear current distribution for a very short

antenna in free space. The other dimensional correction, which has already been noted, is that one uses an effective radius of $\sqrt{2}$ a instead of the actual radius a in all calculations using the filament model.

In most cases, 21 active antenna segments were used. Trials with 33 and 45 segments show only slight changes. It is not at all clear what is an optimum number of segments to use because one cannot always assume that using more terms gives a better approximation.

CHAPTER IV. NUMERICAL DIFFICULTIES

The field expressions for the filament current model appear deceptively simple. Even though these expressions have required a lengthy derivation, most of the effort expended on this problem has been in performing numerical computations. For the terms in closed form, one must guard against loss in accuracy due to subtracting nearly equal terms, and for the terms indicated as integrals, one must perform difficult numerical integrations. The purpose of this section is to describe the numerical analysis required in writing an efficient computer program. Particular attention is paid to the numerical integrations needed for E_{zf}. The general question of stability of the method is discussed in Chapter V.

The computer program that is used can be found in the Appendix. For computational purposes, it was convenient to formulate the field expressions with dielectric constants normalized to ε. Thus, in the program ε' is actually ε'/ε, ε_z is $\varepsilon_z/\varepsilon$, and the field expressions have been correspondingly modified. One result of this renormalization is that one uses $n_1\sqrt{\varepsilon}$ in place of n_1. In this case, one must be careful to compute $n_1\sqrt{\varepsilon}$ as the square root of $n_1^2\varepsilon$ with the negative imaginary part rather than as the product of the square roots of n_1^2 and ε taken individually.

For the singular terms in closed form, E_{zs}, E_{zfs1}, and E_{zfs2}, one must be careful to avoid subtracting nearly equal quantities. This problem increases with increasing distance z. As has been already indicated, if fields are needed more than 30 segments away, the δ-source model gives entirely adequate values. A series expansion of the singular terms has

been made, but the range of validity for the filament and the δ-source models overlap and, therefore, the series expansion is not needed.

The largest source of numerical difficulty is performing the numerical integration for the finite term E_{zf}. The shape of the graph of the integrand varies with the three plasma parameters, the free-space wavenumber k_o, and the distance z. Figure 4 shows real and imaginary parts of the integrand for various parameters scaled so that the difference between maximum and minimum function values is unity. For some plasma parameters the integrand is well-behaved, but for many values, the integrand is nearly singular at some point. The integrand starts at zero, goes through a strong positive peak and through a strong negative peak. Essentially, one has to subtract the effects of the two large and nearly equal peaks. As Y^2 or X gets closer to 1, and as the loss factor Z decreases, the peaks get narrower and steeper until the integrand resembles the doublet function.

Now one can appreciate the numerical difficulty. The standard technique of singularity subtraction is not applicable because of the complicated form of the integrand. One cannot even find analytically the zero crossing of the integrand. An integration scheme with moderate-sized uniform steps might only randomly sample the nearly-singular region or overstep it completely. If the steps were small enough to accurately sample the peaks, there would be an excessive number over regions where the function is relatively flat. Therefore, we have chosen a variable-step Romberg integration scheme [9].

The Romberg quadrature scheme is based on Richardson extrapolation of successive trapezoidal-rule estimates of the area under the integrand. Suppose one needs the integral of some function f(x) over the interval

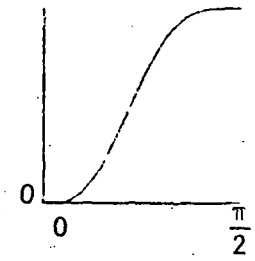

REAL Part, z = 0
X = .1, Y^2 = .1,
Z = .05

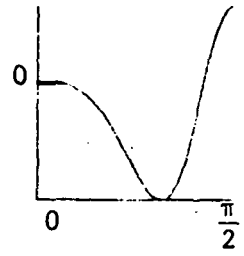

REAL Part, z = 0
X = .3, Y^2 = .5,
Z = .05

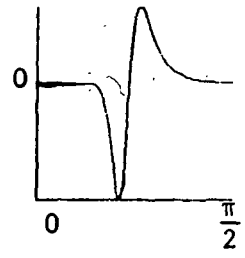

REAL Part, z = 0
X = .7, Y^2 = .5,
Z = .05

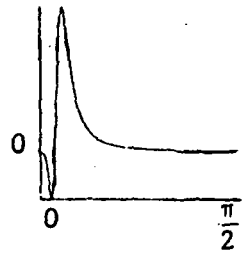

REAL Part, z = 0
X = .9, Y^2 = .9,
Z = .05

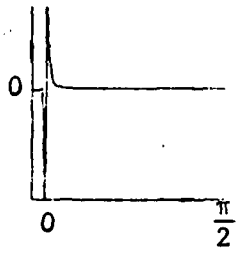

REAL Part, z = 0
X = .9, Y^2 = .9,
Z = .01

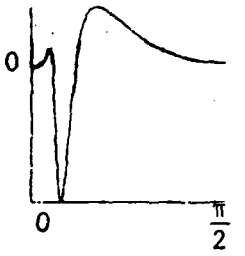

REAL Part, z = π
X = .9, Y^2 = .9,
Z = .05

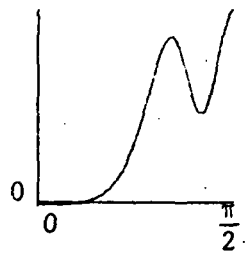

IMAG Part, z = π
X = .3, Y^2 = .7,
Z = .05

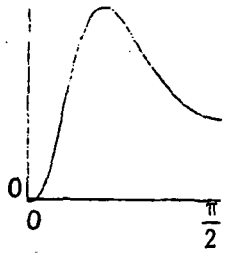

REAL Part, z = 0
X = 1.5, Y^2 = .5,
Z = .05

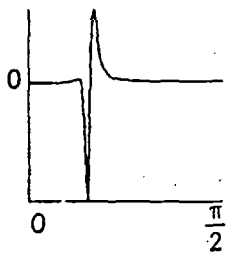

IMAG Part, z = 0
X = 1.9, Y^2 = 1.9,
Z = .05

Figure 4. Normalized Integrand in the Numerical Integration of E_{zf} for Various Plasma Parameters and Distances (k_o = .576, H = π/2, n = 21)

[a, b]. Let h = a - b. The trapezoidal-rule estimate of the area for 2^k equally spaced segments is

$$T_{ok} = \frac{h}{2^k}\left[\frac{1}{2} f(x_o) + f(x_1) + \cdots + f(x_{2^k-1}) + \frac{1}{2} f(x_{2^k})\right] \tag{4.1}$$

where

$$x_n = a + (n - 1)\frac{h}{2^k}.$$

Extrapolations T_{nk} can be generated by the formula

$$T_{nk} = \frac{1}{4^n - 1}(4^n T_{n-1,k+1} - T_{n-1,k}). \tag{4.2}$$

These results can be tabulated as a triangular array

$$\begin{array}{cccc} T_{00} & & & \\ T_{01} & T_{10} & & \\ T_{02} & T_{11} & T_{20} & \\ T_{03} & T_{12} & T_{21} & T_{30} \\ \cdots & & & \end{array} \tag{4.3}$$

The elements of the first column are the trapezoidal-rule estimates; each other element is generated from the element to the left and the element above the element to the left. The accuracy of the estimates becomes better as one moves down and to the right. The procedure stops when the last two elements of a row are sufficiently close. Recall that the trapezoidal rule has an error term on the order of h^3. The application of (4.2) to T_{00} and T_{01} subtracts the h^3 error term leaving only an error on the order of h^5 for T_{10}. Substituting (4.1) into (4.2) shows that T_{10} is exactly the Simpson rule estimate; similarly, T_{20} is the third Newton-Cotes formula. One might suspect that T_{ko} is the k^{th} Newton-Cotes formula, but fortunately that is not true. High-

order Newton-Cotes formulas suffer severely due to round-off error while Romberg's method converges very well.

Due to the particular integrand in this problem, we have partially followed modifications suggested by Miller and Burke [10]. This modification is applicable to any numerical integration where the function is well-behaved except in a small subinterval. The original interval is divided into m subintervals and Romberg's method is applied to each. Convergence is checked by means of a test ratio T_r. If

$$\frac{|T_{01} - T_{10}|}{|T_{10}|} < T_r \tag{4.4}$$

only the midpoint of the subinterval needs to be computed and T_{10} can be used as the area of the subinterval. If (4.4) does not hold, two additional points in the subinterval are computed and the program checks if

$$\frac{|T_{11} - T_{20}|}{|T_{20}|} < T_r .$$

If (4.5) is true, T_{20} is used as the estimate of the area. However, if (4.5) is not satisfied, the program subdivides the interval and applies Romberg's method on that new subinterval rather than subdividing all intervals as the unmodified version would require. Thus, no estimate higher than T_{20} is computed for an interval. This scheme is efficient since the midpoint of the new subinterval has already been calculated. If one had tried using an adaptive Gaussian quadrature scheme, one could not have used any previous calculations. A distinctive feature of our

method is that our program saves all calculations made. Thus when a subinterval converges, one already has the function values for the end points and midpoint of the next subinterval to be integrated. To be practical, one must limit the maximum number of subdivisions allowed and the minimum size of a subinterval.

The exact error of this method is hard to estimate precisely. One may calculate an error estimate as the sum of the differences between the two best area estimates for each subinterval. This is a very pessimistic guess of the error. Even so, in most cases the relative error calculated in this way will be far less than T_r although there is no assurance that this is always true. The usual value used for T_r is 10^{-4}.

A very interesting pathological case exists for this modified integration scheme. The T_{20} estimate term of (4.3) is exact for a polynomial of degree up to 5. When the program tried integrating $y = x^8$ over [0, 1] as a test problem, it kept subdividing the first interval until it had reached the maximum number of subdivisions allowed. The problem is analogous to integrating a parabola with the trapezoidal rule. Consider approximating the function $y = x^2$ with a straight line over $[0, \varepsilon]$. The true value of the integral over the interval will be $\frac{1}{3}\varepsilon^3$ but the integral of the approximation will be $\frac{1}{2}\varepsilon^3$. Clearly the absolute error of the approximation decreases as ε decreases but the relative error does not. When a maximum number of subdivisions is specified, there is no practical problem. Absolute error on the first interval is small enough, and for any interval not containing the 0, the relative error converges. In practice, this pathology occurs when the function behaves as a high-order polynomial.

The Romberg method has been described for the case of a real function. For a complex function, such as in this problem, we have required that the test ratio be satisfied for both the real and imaginary parts of the estimates before going to the next interval.

The integration of E_{zf} is done slightly differently than formally indicated. The integrands of P_{n1} and P_{n2} are added together before integrating. This not only eliminates the need for two separate applications of Romberg's method, but also simplifies the handling of terms common to P_{n1} and P_{n2}.

CHAPTER V. STABILITY OF METHOD OF MOMENTS

After many trial runs, we wished to test the stability of our method. Even if the models used were perfect and electric fields could be precisely analytically formulated, there would still be computational errors that would be transmitted to the final answers. Knowing the sensitivity of the final answers to both matrix manipulation errors and errors in computing the fields allows one to estimate how accurately fields must be calculated to get results that are reliable. Early results obtained from field calculations with deliberate perturbations showed a noticeable sensitivity. The stability theory developed here applies not only to this particular plasma problem, but also to any problem using the method of moments.

This sensitivity analysis will use norms of complex vectors and matrices to estimate error. Because of the wide variety in definitions of matrix norms, we wish to develop our analysis in detail and carefully define our matrix and vector notation for complex matrices and vectors. Our definition will follow Forsythe and Moler [11].

All vectors x will be assumed to be column vectors. A^T and x^T will indicate the transpose of matrix A and vector x, that is, the original matrix or vector with rows and columns interchanged. A^H and x^H will indicate the matrix or vector that is the complex conjugate of the transpose of the original matrix or vector. A matrix that is equal to its own transpose conjugate is said to be Hermitian.

Next we define vector norms. The Euclidean norm of a complex vector x is defined as

$$||x||_2 = \sqrt{x^H x} \quad \sqrt{|x_1|^2 + |x_2|^2 + \cdots + |x_n|^2} \tag{5.1}$$

where $x_1, x_2, \cdots, x_n$ are components of x. For real vectors this norm is the usual concept of the length of a vector. We can also define vector norms

$$||x||_1 = \sum_{i=1}^{n} |x_i| \tag{5.2}$$

$$||x||_\infty = \max_{1\leq i\leq n} |x_i|. \tag{5.3}$$

These norms are not quite as geometrically obvious as the Euclidean norm. Figure 5 shows all possible unit-length vectors in two dimensions for each of the three norms. Mathematically, one can define an infinite number of norms, but these three are the most useful. All vector norms must satisfy the following three properties.

$$||cx|| = |c| \cdot ||x|| \qquad \text{for any real scalar } c, \tag{5.4}$$

$$||x|| \geq 0 \text{ and } ||x|| = 0 \qquad \text{if and only if } x = \text{null vector}, \tag{5.5}$$

$$||x + y|| \leq ||x|| + ||y|| \qquad \text{(triangle inequality)}. \tag{5.6}$$

Next we define a matrix norm for square matrices A as

$$||A|| = \max_{x\neq 0} \frac{||Ax||}{||x||} \tag{5.7}$$

or equivalently

$$||A|| = \max_{||x||=1} ||Ax||. \tag{5.8}$$

Each of the three vector norms thus produces a matrix norm that is said to be compatible with the generating vector norm. Because of this compatibility, these matrix norms satisfy the three vector norm

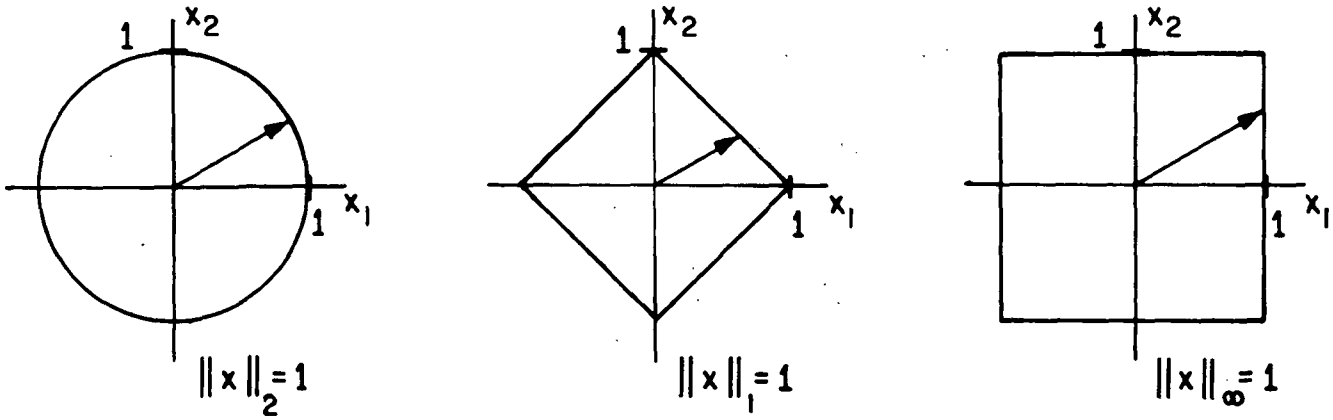

Figure 5. Unit Vectors under Different Norms

properties (5.4), (5.5), and (5.6), when x and y are replaced by matrices. From the definition (5.7) one can see

$$||Ax|| \leq ||A|| \cdot ||x|| \quad \text{for all A and x.} \tag{5.9}$$

The main advantage of the two non-Euclidean norms is their ease of computation. It can be shown [12] that

$$||A||_1 = \max_{1\leq j\leq n} \sum_{i=1}^{n} |a_{ij}| \tag{5.10}$$

$$||A||_\infty = \max_{1\leq i\leq n} \sum_{j=1}^{n} |a_{ij}|. \tag{5.11}$$

Finally we can introduce a scalar function of a matrix that measures the degree of ill-conditioning for certain operations with this matrix.

Define the condition number of square matrix A as

$$\text{cond } (A) = ||A|| \cdot ||A^{-1}||. \tag{5.12}$$

For real matrices, the condition number with respect to the Euclidean norm can be calculated

$$\text{cond}_2(A) = \sqrt{\lambda_1/\lambda_n} \tag{5.13}$$

where λ_1 and λ_n are the largest and smallest eigenvalues in absolute magnitude of the symmetric matrix AA^T. If matrix A is symmetric

$$\text{cond}_2(A) = \frac{|\lambda_1|}{|\lambda_n|} \tag{5.14}$$

where λ_1 and λ_n are the largest and smallest eigenvalues of A.

If matrix A is complex, (5.13) can be applied where one uses the largest and smallest eigenvalues of AA^H which will be Hermitian and thus have real eigenvalues.

For the case of real symmetric matrices and the Euclidean norm, one can most easily understand the application of the condition number. One can think of premultiplication by a matrix as a vector function in which components of the vector in the direction of the eigenvectors of the matrix are stretched or shrunk by the respective eigenvalues. Consider $y = Ax$ as a mapping of vectors x onto vectors y. It is geometrically clear that $y = Ax$ maps the n-dimensional sphere of all unit length x's onto an n-dimensional ellipsoid with semi-major axis λ_1 and semi-minor axis λ_n. One can see that $|\lambda_1|/|\lambda_n|$ is the ratio of possible distortions a vector x can undergo. Also note that the condition number shows the loss in accuracy for computation of components of x that are not in the direction of the eigenvector associated with the largest eigenvalue. The geometrical interpretation with other norms is not as clear.

It is to be stressed that cond(A) is a far better measure of ill-conditioning than the smallness of the determinant A. Even if A is normalized, the smallness of det(A) has a weak relation to the degree of ill-conditioning. Supporting examples are given by Forsythe and Moler.

Now we will indicate how the condition number can be used to measure sensitivity of a solution to a linear system. Consider the problem

$$Ax = y \tag{5.15}$$

with unknown vector x. Suppose now that y is precisely known but that

A and, therefore, x are subject to uncertainty. Then

$$(A + \delta A)(x + \delta x) = y \tag{5.16}$$

where δA and δx are uncertainties in A and x. Forsythe and Moler show from Equations (5.4) to (5.9) that

$$\frac{||\delta x||}{||x + \delta x||} \leq \text{cond } (A) \frac{||\delta A||}{||A||} . \tag{5.17}$$

Thus we can relate relative uncertainty in A to relative uncertainty in x by a function of A itself. It should be noted that (5.17) is the sharpest inequality possible; i.e., the equality will occur for some δA. Recall that any of the three norms can be used in (5.17). Occasionally it is useful to write (5.17) as

$$\frac{||\delta x||}{||x + \delta x||} \leq ||A^{-1}|| \cdot ||\delta A||. \tag{5.18}$$

To make practical calculations of the condition number, the condition number based on the infinity norm has been used. Equation (5.10) shows that the norm of A is the sum of the magnitudes of the elements of the row that gives the maximum sum. For the special form of the impedance matrix Z, this is always the center row. For the inverse matrix Z^{-1}, in general, one must check all the rows above and including the center row. However, if k_o is small and the current distribution is essentially triangular, then the center row will have the maximum sum of the magnitude of the elements. Multiplying the norm of Z by the norm of Z^{-1} gives the condition number which determines maximum error for the current on any segment. It should be noted

that since Z and Z^{-1} are symmetric, $\text{cond}_\infty(Z) = \text{cond}_1(Z)$. Thus, if one estimates error in Z as $||\delta Z||_1$, one can use the same condition number to measure relative error in current I as $||\delta I||_1 / ||I + \delta I||_1$.

Although the use of the Euclidean norm is geometrically clearer, it requires far more computations. First, one must form the Hermitian matrix ZZ^H before finding eigenvalues. This multiplication, in itself, takes on the order of n^3 multiplications. Rather than finding all the eigenvalues, one needs to find only the largest and smallest. A computer program has been written to find the largest eigenvalue by iteration. The iteration scheme operates on the principle that successive premultiplications of a vector by a matrix orients the resulting vector in the direction of the eigenvector associated with the largest eigenvalue in magnitude. Each iteration takes on the order of n^2 operations and the convergence of this scheme is so poor that the convergence can be hastened by a linear extrapolation of two successive vectors. Finding the minimum eigenvalue is even harder. All of the eigenvalues of a matrix can be shifted by subtracting the maximum eigenvalue from the diagonal, thus making the former minimum eigenvalue the new maximum eigenvalue in magnitude. This, however, does not appear to be an efficient numerical procedure because small eigenvalues tend to be close together causing slow convergence. Even worse, more accuracy is required so that when the largest eigenvalue is added to the final answer to obtain the true minimum eigenvalue, all significant figures are not lost. One can invert the matrix and find the maximum eigenvalue of that matrix. This eigenvalue will be the reciprocal of the minimum eigenvalue of the original matrix, but the inversion itself will take on the order of n^3 operations. All considered, using the

infinity norm, which is easy to calculate and gives the error in a Chebyshev sense, appears to be more practical.

CHAPTER VI. RESULTS

Current distributions and antenna impedances have been calculated for various plasma parameters. Tables 2 through 9 and Figures 7 through 14 give the results for eight different plasma conditions. A graph with axes X and Y^2 is very useful for mapping plasma conditions. (See Figure 6.) The lines plotted on this graph correspond to various resonances in a lossless plasma. When dispersion surfaces are drawn over this plot, this display is known as a CMA diagram [13]. From this display one can see that the nature of the characteristic waves in the plasma changes abruptly as one crosses any one of these lines; hence, these lines form regions with similar properties. Each region has been sampled in the results presented. For our formulation, it is necessary to have some collision loss; therefore, for all cases, except for free space which corresponds to $X = 0$ and $Y^2 = 0$, Z has been arbitrarily set to .05. In each case $H = 1$, $a = 1/250$, and results are presented for three values of k_o. Since there is symmetry around the center feed, the graphs of current distribution show the current from the end point to the feed. The condition number based on the infinite norm, as described in the last chapter, is presented with each calculation.

Balmain has developed an analytical expression for the input impedance using a quasi-static approximation which assumes a linear current distribution [14]. The impedance predicted by Balmain's formulation is presented for comparison. Where our method has determined a linear current distribution, the two values should agree.

The first case presented is the degenerate plasma condition of free space. (See Table 2 and Figure 7.) One can see that the data

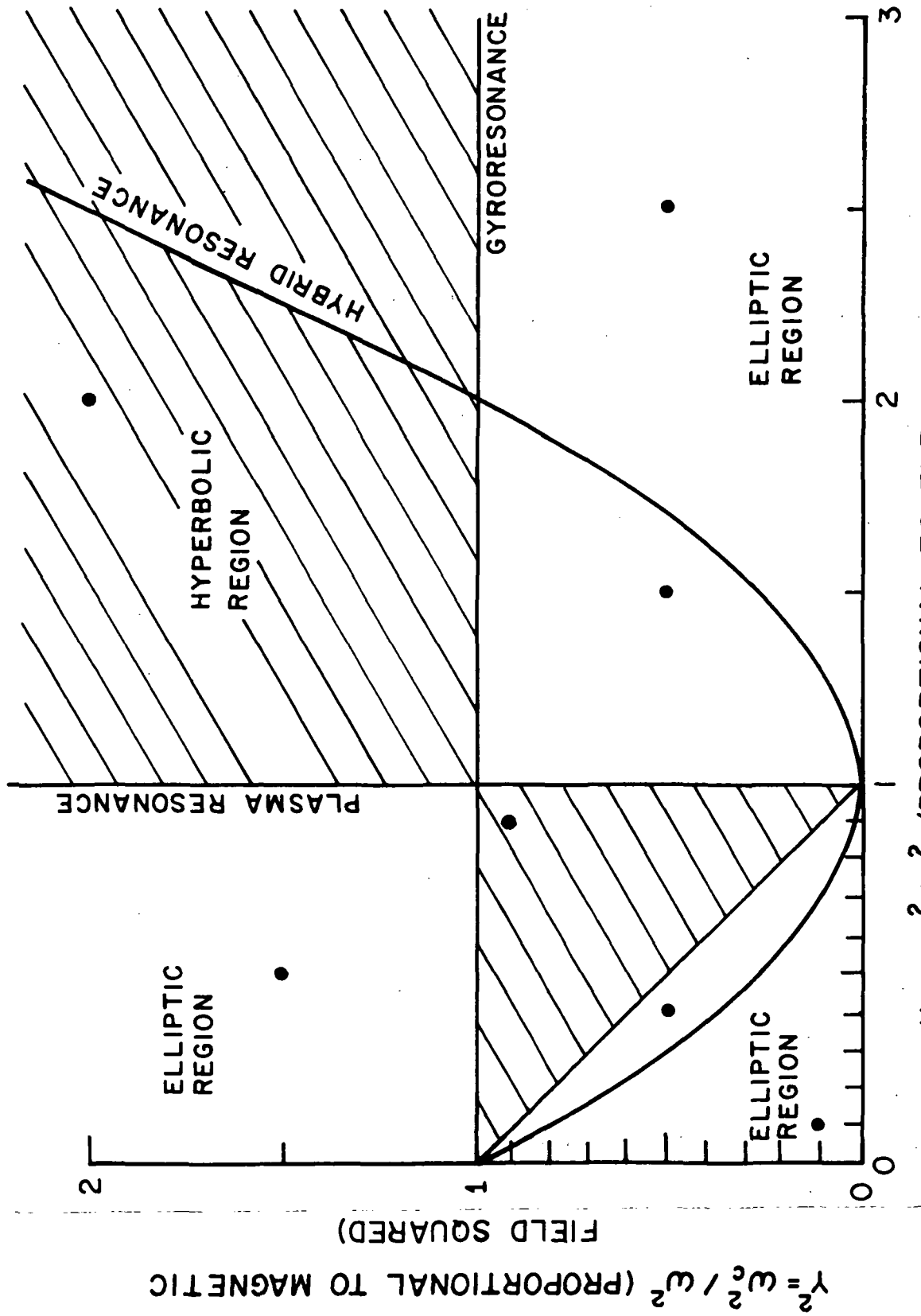

Figure 6. Plasma Parameter Diagram Showing Cases Run

TABLE 2.

FREE-SPACE RESULTS ($X = 0$, $Y^2 = 0$, $Z = 0$)

(See Figure 7)

$\varepsilon = 1.0$ $\varepsilon' = 0$ $\varepsilon_z = 1.0$

$k_o (m^{-1})$	IMPEDANCE (OHM) — COMPUTED	ADMITTANCE (MILLIMHO) — COMPUTED	$COND_\infty$
.1	.1600 - j 4491.	7.937×10^{-6} + j .2227	27.1
.75	10.39 - j 471.4	4.671×10^{-2} + j 2.120	35.8
1.5	68.86 + j 16.52	13.73 - j 3.295	139

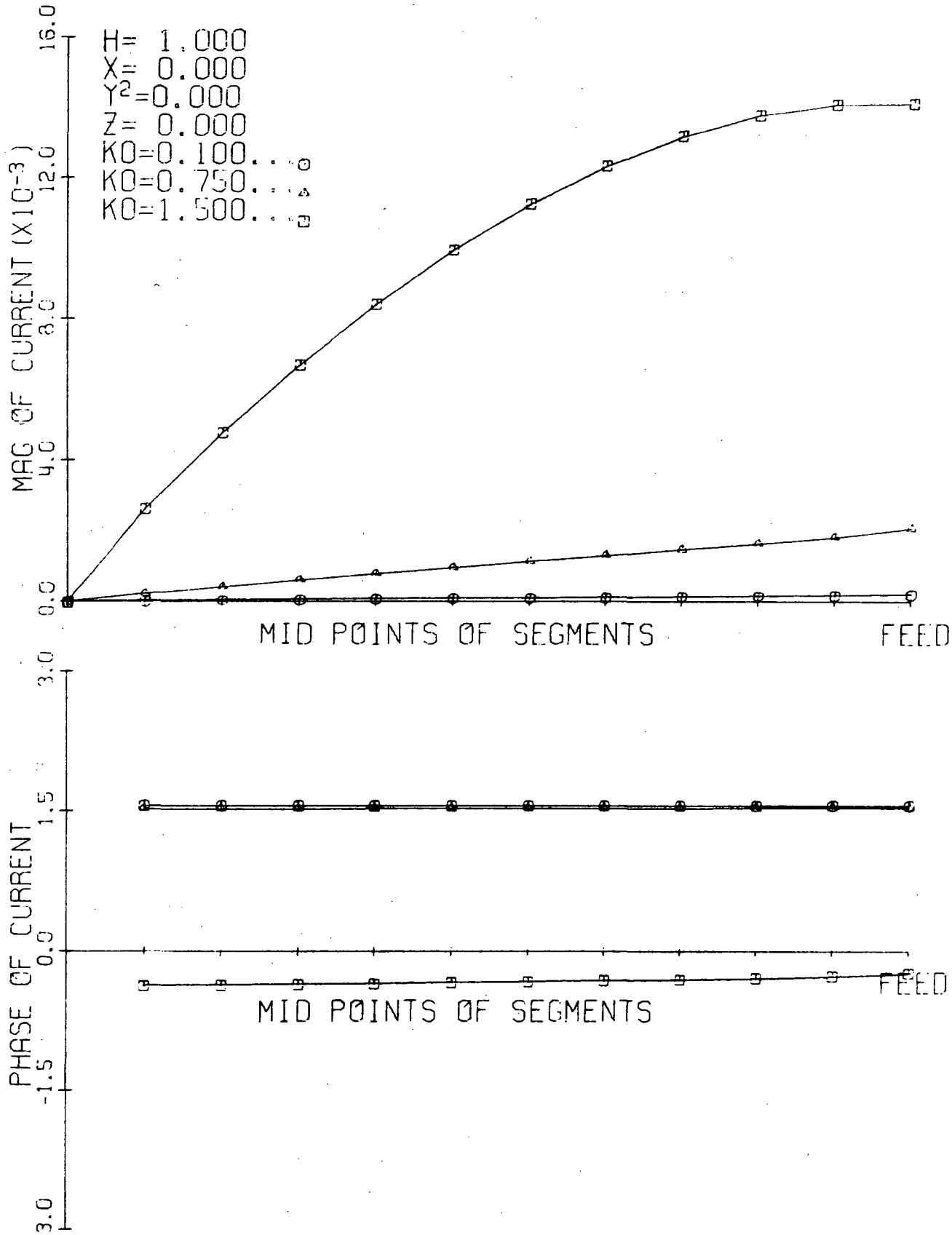

Figure 7. Current Distribution for Free Space (X = 0, Y^2 = 0, Z = 0)

TABLE 3.

UNDERDENSE ELLIPTIC PLASMA RESULTS ($X = .1$, $Y^2 = .1$, $Z = .05$)

(See Figure 8)

$\varepsilon = .8893 - j\ 6.760 \times 10^{-3}$ $\quad \varepsilon' = .0348 + j\ 3.878 \times 10^{-3}$ $\quad \varepsilon_z = .9002 - j\ 4.988 \times 10^{-3}$

$k_o (m^{-1})$	IMPEDANCE (OHM)		ADMITTANCE (MILLIMHO)		$Cond_\infty$
	Computed	Balmain	Computed	Balmain	
.1	38.57 - j 5051.	44.92 - j 6092.	$1.512 \times 10^{-3} + j\ .1980$	$1.210 \times 10^{-3} + j\ .1641$	27.1
.75	14.84 - j 547.2	5.989 - j 812.3	$4.953 \times 10^{-2} + j\ 1.826$	$9.075 \times 10^{-3} + j\ 1.2331$	34.5
1.5	63.02 - j 31.88	2.994 - j 406.2	12.64 + j 6.392	$1.815 \times 10^{-2} + j\ 2.462$	151.

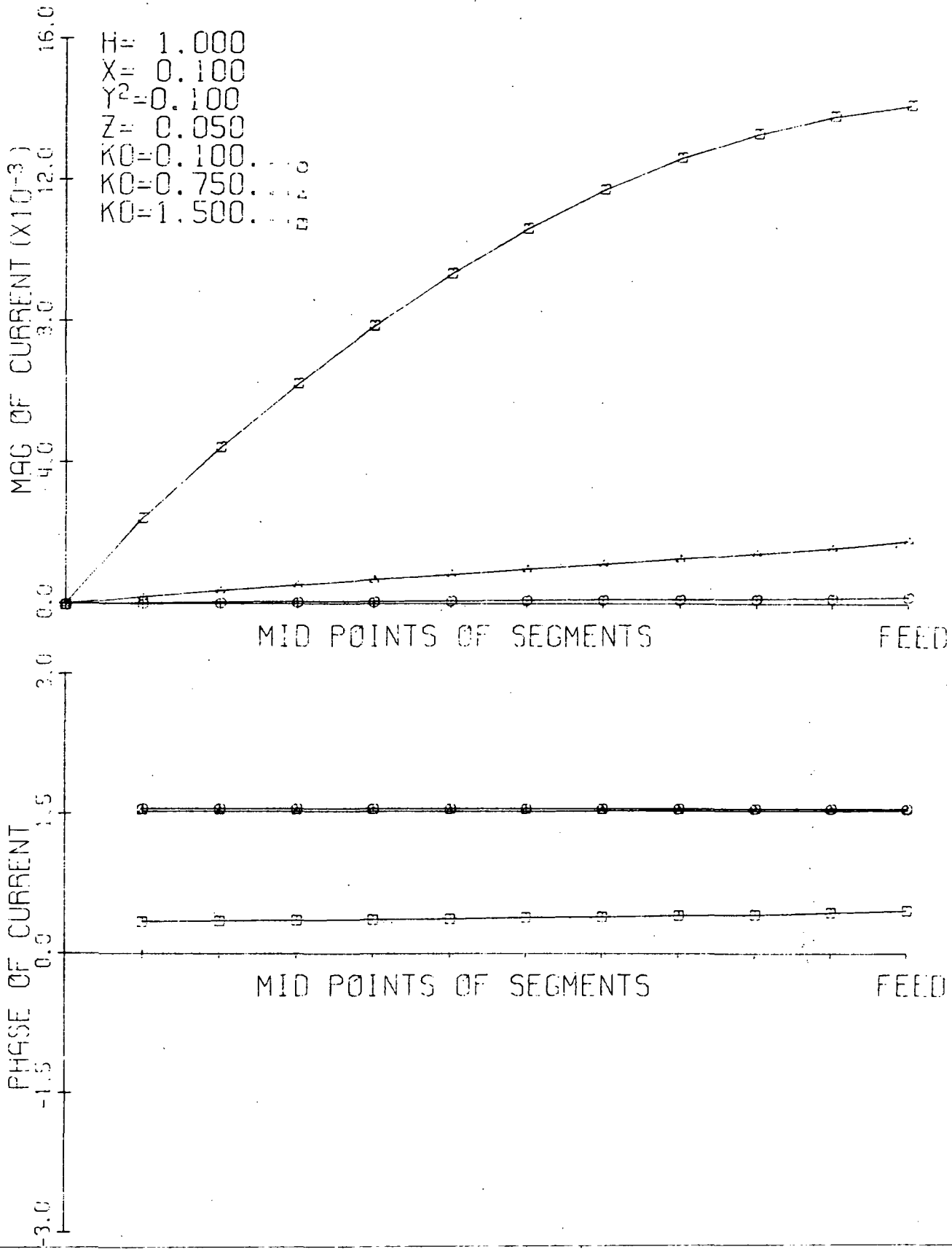

Figure 8. Current Distribution for Underdense Elliptic Plasma (X = .1, Y^2 = .1, Z = .05)

TABLE 4.

UNDERDENSE ELLIPTIC PLASMA RESULTS ($X = .4$, $Y^2 = .5$, $Z = .05$)

(See Figure 9)

$\varepsilon = .2194 - j\ .1167$ $\qquad$ $\varepsilon' = 5.464 + j\ .1098$ $\qquad$ $\varepsilon_z = .6610 - j\ 1.995 \times 10^{-2}$

$k_o (m^{-1})$	IMPEDANCE (OHM)		ADMITTANCE (MILLIMHO)		$Cond_\infty$
	Computed	Balmain	Computed	Balmain	
.1	8216. - j 1581.	8277. - j 17910.	$2.588 \times 10^{-2} + j\ 4.980 \times 10^{-2}$	$2.127 \times 10^{-5} + j\ 4.601 \times 10^{-2}$	26.8
.75	1096. - j 1988.	1104. - j 2388.	.2126 + j .3857	$1.595 \times 10^{-4} + j$ .3451	28.3
1.5	572.7 - j 806.4	551.8 - j 1194.	.5854 + j .4243	$3.190 \times 10^{-4} + j$ .6902	32.3

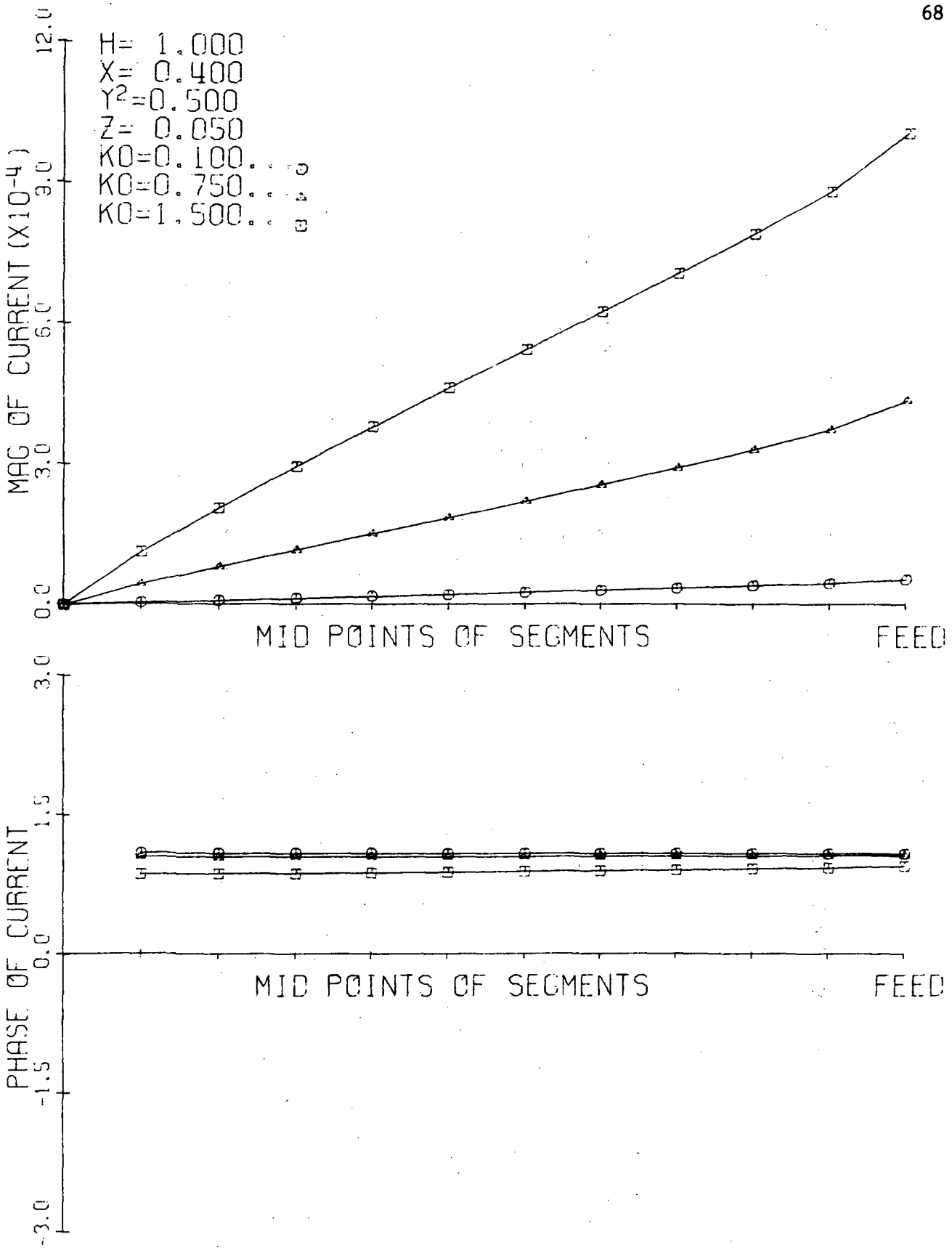

Figure 9. Current Distribution for Underdense Elliptic Plasma (X = .4, Y^2 = .5, Z = .05)

TABLE 5.

UNDERDENSE HYPERBOLIC PLASMA RESULTS ($X = .9$, $Y^2 = .9$, $Z = .05$)

(See Figure 10)

$\varepsilon = -3.729 - j\ 4.389$ $\qquad \varepsilon' = -1.059 + j\ 7.258 \times 10^{-2}$ $\qquad \varepsilon_z = -5.555 \times 10^{-2} + j\ 1.858 \times 10^{-2}$

$k_o (m^{-1})$	IMPEDANCE (OHM)		ADMITTANCE (MILLIMHO)		Cond $_\infty$
	Computed	Balmain	Computed	Balmain	
.1	612.9 + j 541.0	1157. + j 728.2	.9171 - j .8095	.6192 - j .3899	26.4
.75	138.3 + j 182.9	154.2 + j 97.09	2.630 - j 3.478	4.644 - j 2.924	11.7
1.5	119.5 + j 164.9	77.10 + j 48.55	2.881 - j 3.976	9.289 - j 5.848	6.34

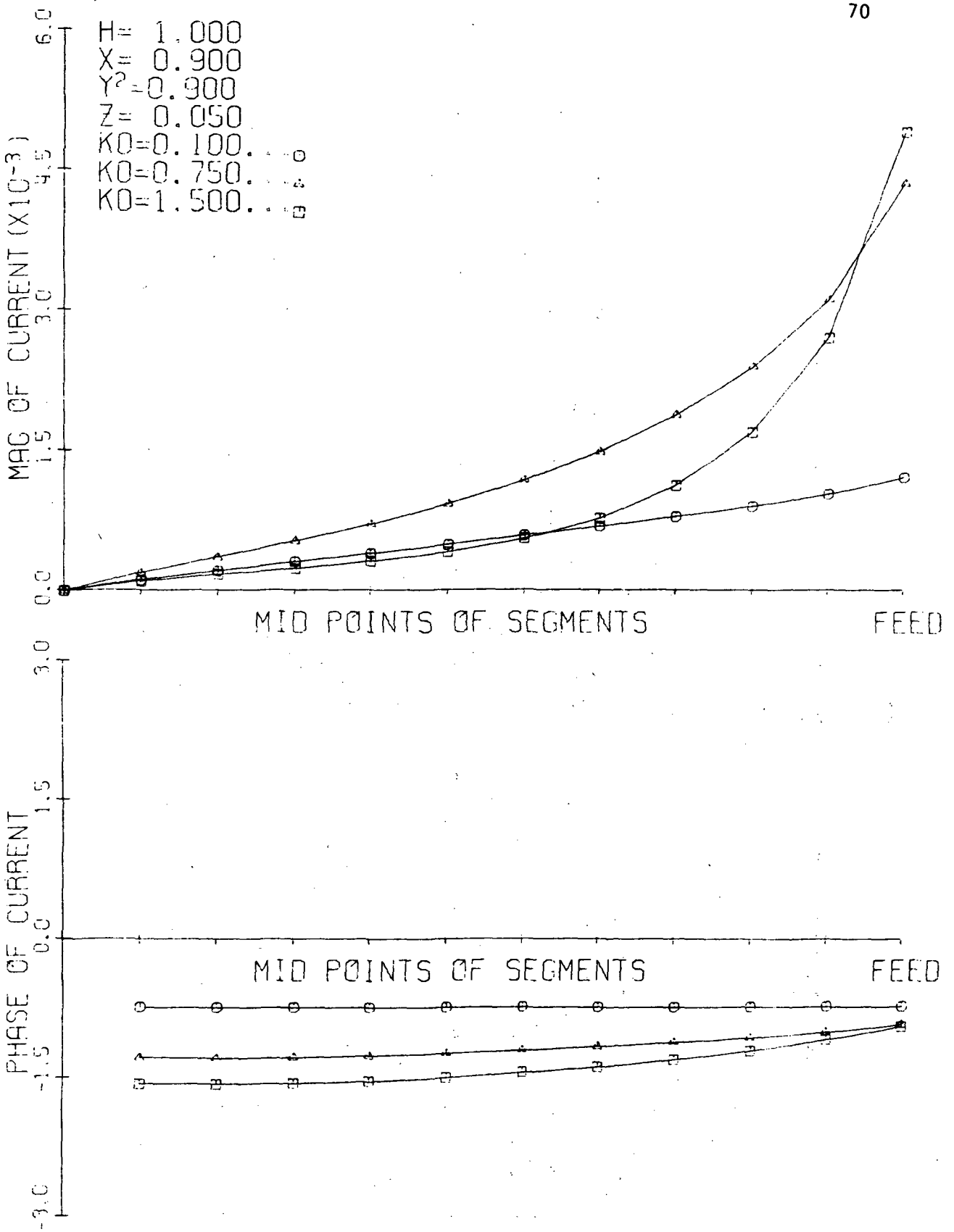

Figure 10. Current Distribution for Underdense Hyperbolic Plasma (X = .9, Y^2 = .9, Z = .05)

TABLE 6.

UNDERDENSE ELLIPTIC PLASMA RESULTS ($X = .5$, $Y^2 = 1.5$, $Z = .05$)

(See Figure 11)

$\varepsilon = 1.948 - j\ 0.2383$ $\quad \varepsilon' = -1.172 + j\ .2333$ $\quad \varepsilon_z = .5103 - j\ .02494$

$k_o (m^{-1})$	IMPEDANCE (OHM)		ADMITTANCE (MILLIMHO)		$Cond_\infty$
	Computed	Balmain	Computed	Balmain	
.1	282.2 - j 2286.	364.7 - j 3161.	$5.321 \times 10^{-2} + j\ .4309$	$3.601 \times 10^{-2} + j.3122$	27.4
.75	64.56 - j 145.8	48.62 - j 421.5	2.540 - j 5.735	.2701 + j 2.341	57.2
1.5	387.4 + j 246.1	24.31 - j 210.8	1.839 - j 1.168	.5401 + j 4.683	36.9

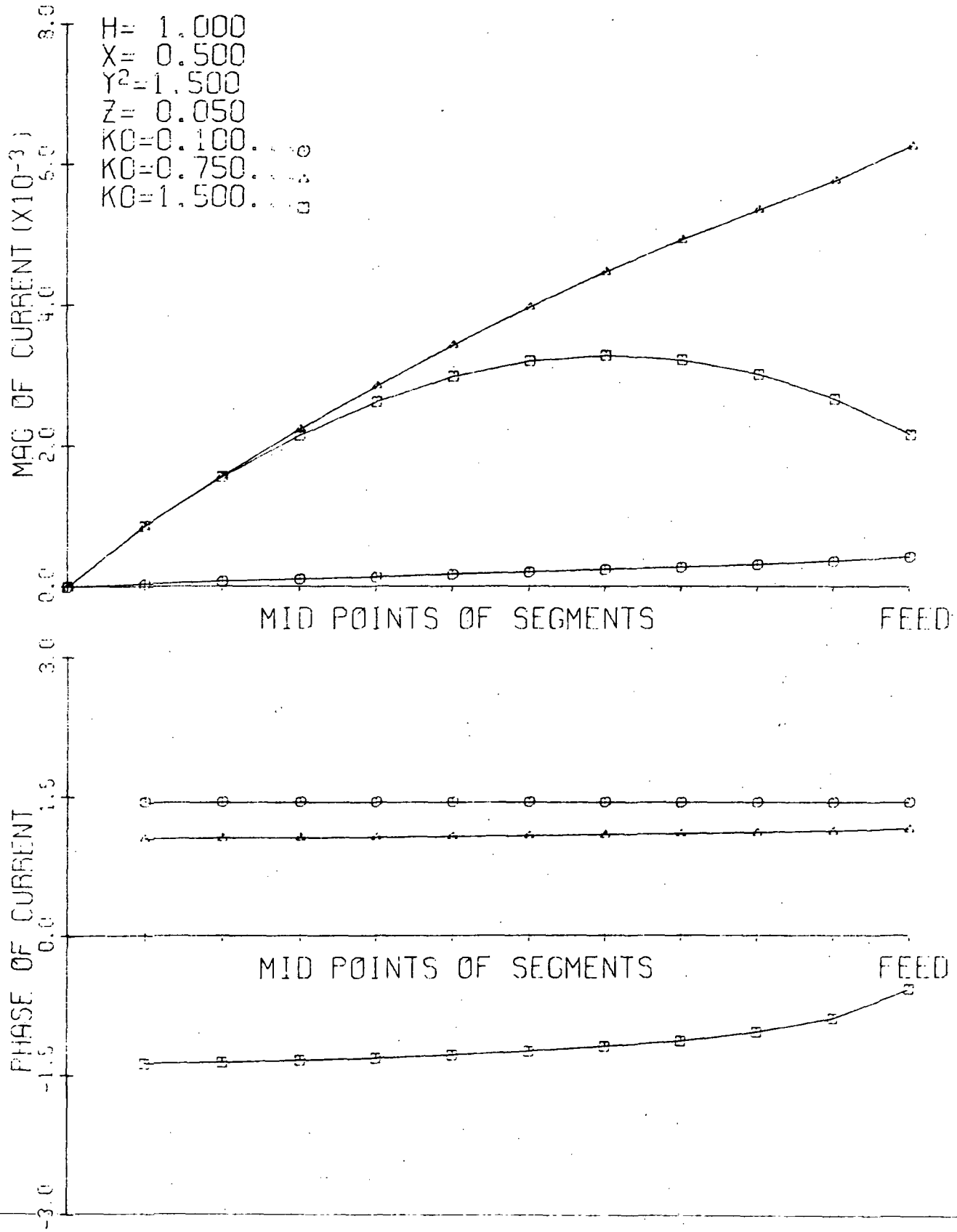

Figure 11. Current Distribution for Underdense Elliptic Plasma (X = .5, Y^2 = 1.5, Z = .05)

TABLE 7.

OVERDENSE ELLIPTIC PLASMA RESULTS ($X = 1.5$, $Y^2 = .5$, $Z = .05$)

(See Figure 12)

$\varepsilon = -1.927 - j\ .4376$ $\quad \varepsilon' = 2.045 - j\ .4119$ $\quad \varepsilon_z = .4963 - j\ 7.481 \times 10^{-2}$

$k_o (m^{-1})$	IMPEDANCE (OHM)		ADMITTANCE (MILLIMHO)		$Cond_\infty$
	Computed	Balmain	Computed	Balmain	
.1	510.2 + j 2268.	687.3 + j 3088.	$9.435 \times 10^{-2} - j\ .4196$	$6.785 \times 10^{-2} - j\ .3089$	26.9
.75	71.67 + j 422.4	90.44 + j 411.8	.3904 - j 2.301	.5089 - j 2.317	18.5
1.5	45.74 + j 328.3	45.22 + j 205.9	.4163 - j 2.988	1.018 - j 4.634	11.0

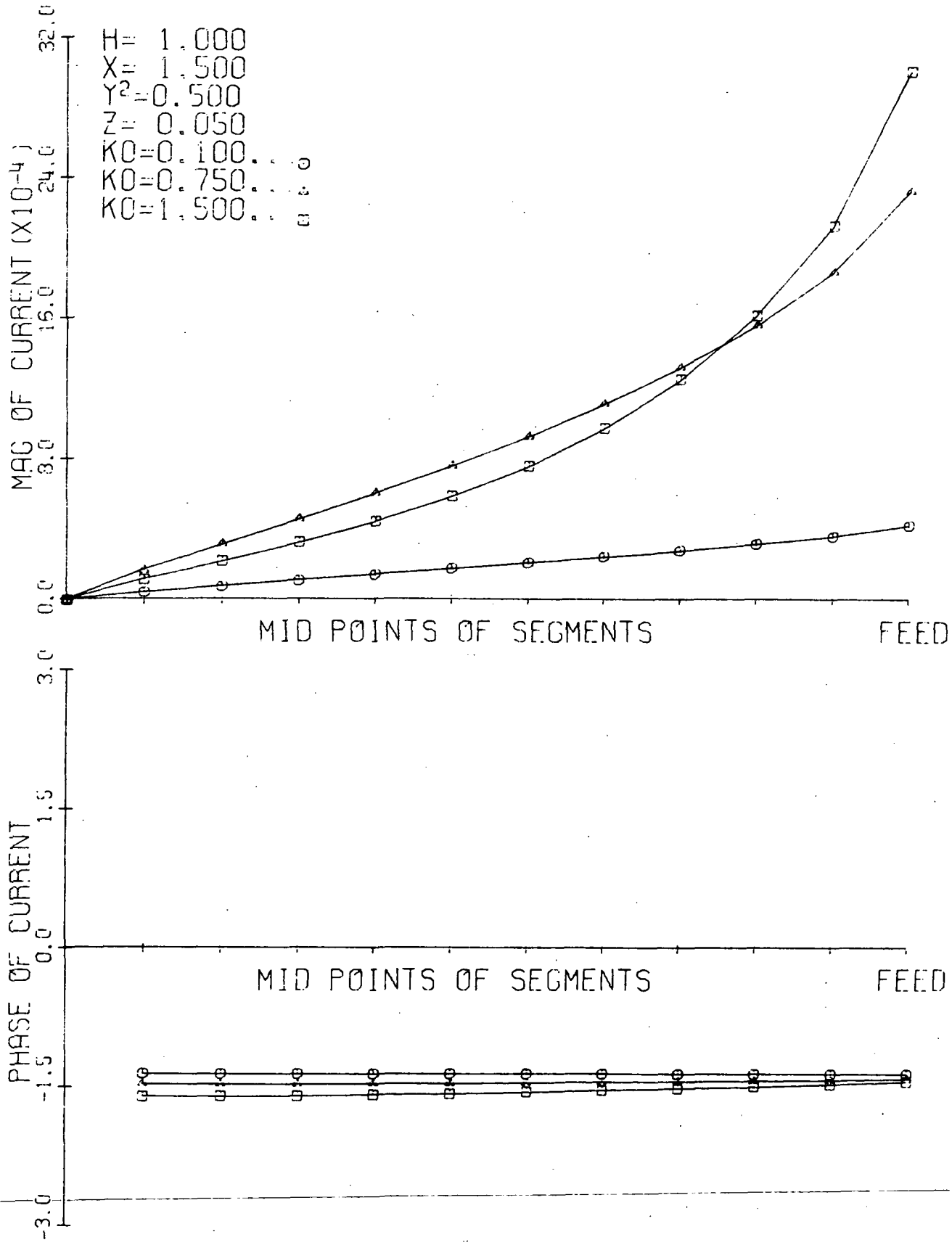

Figure 12. Current Distribution for Overdense Elliptic Plasma (X = 1.5, Y^2 = .5, Z = .05)

TABLE 8.

OVERDENSE ELLIPTIC PLASMA RESULTS ($X = 2.5$, $Y^2 = .5$, $Z = .05$)

(See Figure 13)

$\varepsilon = -3.876 - j\ .7294$ $\qquad$ $\varepsilon' = 3.415 + j\ .6865$ $\qquad$ $\varepsilon_z = -1.494 - j..1247$

$k_o(m^{-1})$	IMPEDANCE (OHM)		ADMITTANCE (MILLIMHO)		$Cond_\infty$
	Computed	Balmain	Computed	Balmain	
.1	212.4 + j 1151.	266.0 + j 1497.	.1544 - j .8394	.1147 - j .6469	26.7
.75	31.29 + j 252.1	35.46 + j 194.8	.4847 - j 3.906	.8609 - j 4.852	15.0
1.5	22.27 + j 208.1	17.73 + j 99.71	.5086 - j 4.752	1.721 - j 9.703	8.16

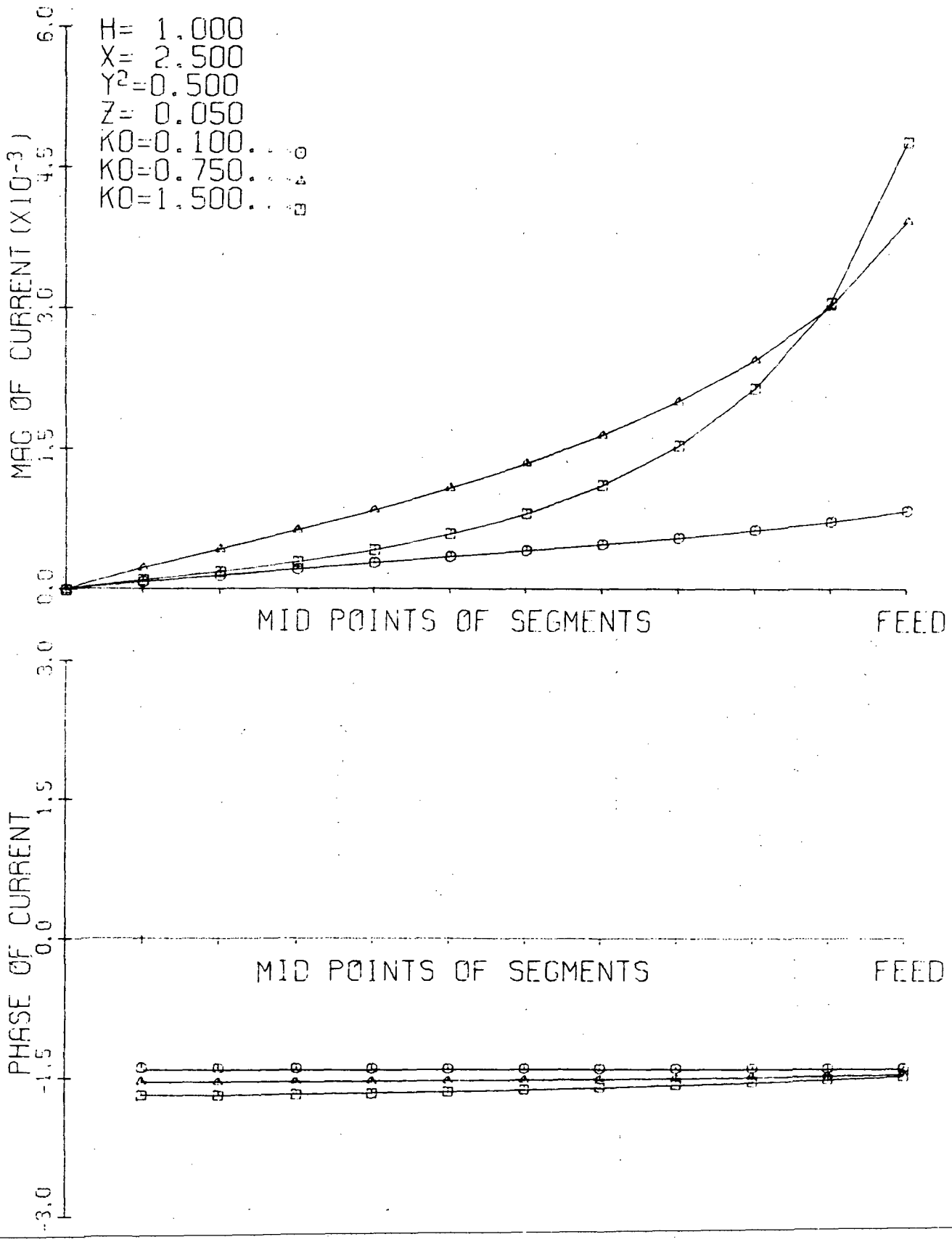

Figure 13. Current Distribution for Overdense Elliptic Plasma (X = 2.5, Y^2 = .5, Z = .05)

TABLE 9.

OVERDENSE HYPERBOLIC PLASMA RESULTS ($X = 2.$, $Y^2 = 2.$, $Z = .05$)

(See Figure 14)

$\varepsilon = 2.9655 - j\ .2958$ $\qquad$ $\varepsilon' = -.9420 + j\ 0.0$ $\qquad$ $\varepsilon_z = -.3289 - j\ .6644$

$k_o(m^{-1})$	IMPEDANCE (OHM)		ADMITTANCE (MILLIMHO)		$Cond_\infty$
	Computed	Balmain	Computed	Balmain	
.1	147.1 - j 1516.	792.0 - j 1972.	$6.340 \times 10^{-2} + j\ .6534$	.1754 + j .4367	27.7
.75	-23.27 - j 21.73	105.6 - j 262.9	22.96 + j 22.43	1.316 + j 3.276	20.3
1.5	-3180. - j 1872.	52.79 - j 131.4	-.2335 + j .1375	2.632 + j.6.551	67.6

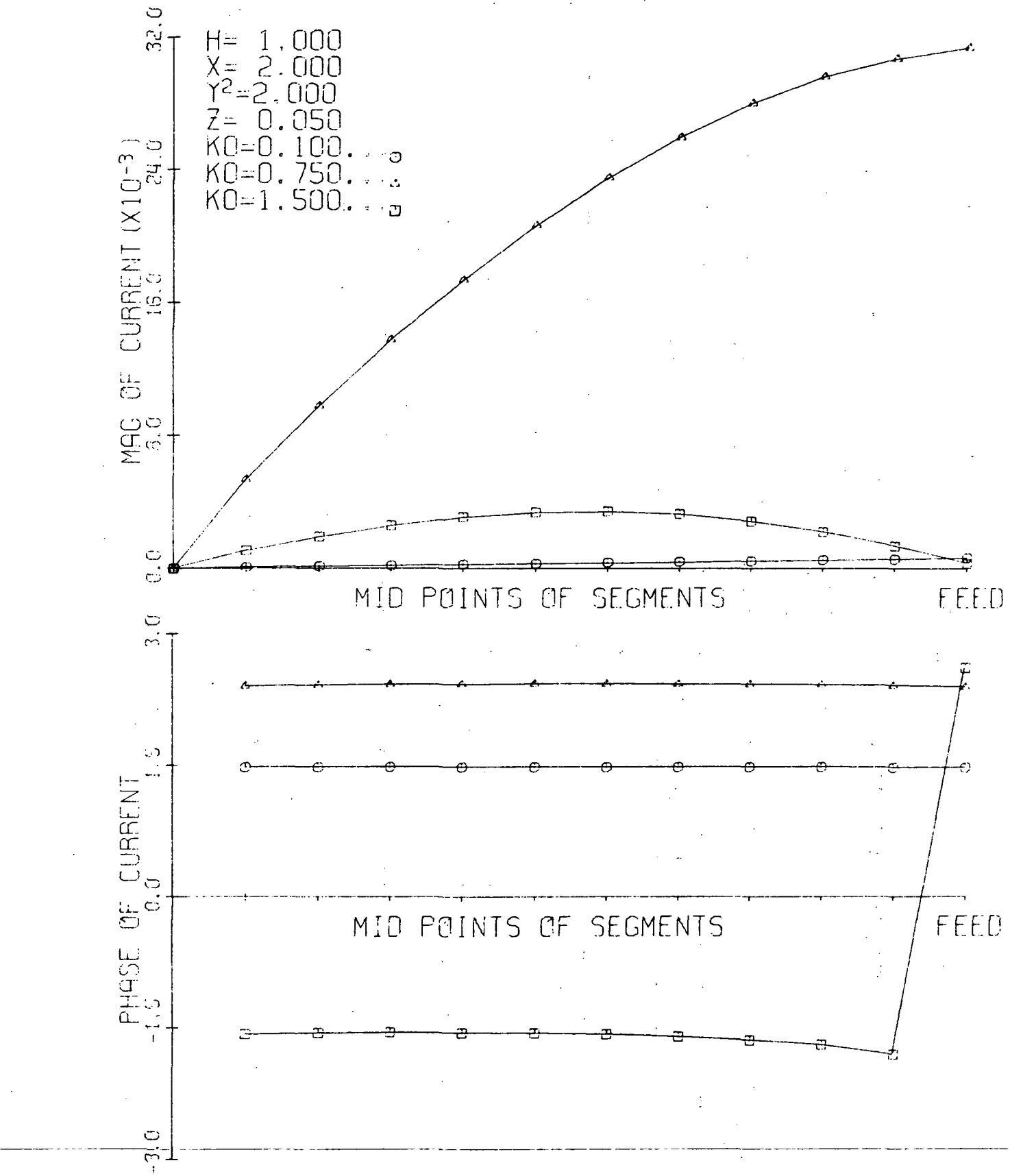

Figure 14. Current Distribution for Overdense Hyperbolic Plasma (X = 2., Y^2 = 2.,Z = .05)

agree generally with well-known results. The condition number for the impedance matrix Z is alarmingly high. For $k_o = 1.5$, which corresponds to a dipole slightly longer than a half wavelength, the condition number is 140. This means that an error of .1 per cent in formulating the self term could cause a 14 per cent error in the input impedance. One should be aware that for free space the Green's function is much simpler and allows one to use better expansion functions in the method of moments. Mautz [15] and Klock [16] have done computer work for more arbitrarily shaped, thin-wire structures that agrees better with measurements than our results for free space. However, condition numbers for some of these results are still high.

Results for anisotropic plasmas are given in Tables 3 through 9 and Figures 8 through 14. The validity of results varies with the region. Although there is not a unique wavelength in an anisotropic plasma, in several cases the current distribution looks like a frequency-scaled, free-space current distribution. Results appear best in regions which make an antenna look shorter, and worse in regions which make an antenna appear longer, just as in free space the stability was best for short antennas. For example, when $H = 1$ and $k_o = 1.5$, an antenna in free space is approximately half-wave resonant, but an antenna in a plasma with $X = 2$ and $Y^2 = 2$ is approximately full-wave resonant. When the current distribution is no longer linear, Balmain's approximation is no longer valid and there is no standard analytical approximation.

Several regions require special comment. In the overdense hyperbolic region, our results predict a negative radiation resistance for $k_o = 7.5$ and 1.5, which is clearly incorrect. The overdense elliptic

region ($X > 1$, $Y^2 < 1$) is more believable but has some unusual properties. The current decreases rapidly from the feed, making the current distribution curve concave upward, the reverse of the usual curvature of a sinusoidal distribution. The condition numbers indicate a much better conditioned problem than free space. Unlike other regions, the condition number decreases and the impedance agrees better with Balmain's approximation as k_o increases, although the current distribution is moving away from the assumed linear distribution. In general, regions separated only by a hybrid frequency resonance show no drastic changes.

There is little experimental work on current distribution which can be compared to our theoretical results. Some work was done by Snyder and Mittra [17], but they were unable to accurately determine the plasma parameters. An attempt was made to compare our results to work done by Ishizone et al. [18]. Their results did not indicate their antenna radius or a plasma loss parameter Z and so our computations were made with an arbitrary H/a ratio of 250 and a Z parameter of .05. Their measurements are all for overdense plasmas (X from 4. to 50) but in both elliptic and hyperbolic regions (Y^2 from 0 to 1.04). In all cases their current distributions have standing-wave characteristics, often with the current increasing at the feed. However, for all of their cases for which we have made computations, our current distribution simply decreases rapidly from the feed similar to our computed results for $X = 2.5$, $Y^2 = .5$. Thus, there is rather poor qualitative agreement between our results and their measurements.

In trying to understand why blatantly incorrect answers are sometimes obtained, one can note certain patterns between the condition number, the validity of the impedance, and the relative importance of the four terms of the Green's function E_z. (See Tables 10, 11, and 12.)

TABLE 10.

ELECTRIC FIELD CALCULATIONS FOR H = 1., k_o = .1, a = $\frac{1}{250}$, X = .1,
Y^2 = .1, Z = .05

FIELD ELEMENTS NO.	EZS		EZFS1/EZFS2		EZF		SUM	
1	-0.3028E 05	0.4002E 07	-0.6989E-01	-0.1542E 03	-0.1887E 00	0.6918E-03	-0.3028080E 05	0.4001714E 07
			0.6168E-02	-0.2459E-01				
2	0.1341E 05	-0.1774E 07	-0.5300E-03	-0.3764E 02	-0.1887E 00	0.1273E-02	0.1341291E 05	-0.1773617E 07
			0.5689E-04	-0.8558E-04				
3	0.1104E 04	-0.1454E 06	-0.4318E-04	-0.1764E 02	-0.1887E 00	0.1853E-02	0.1103970E 04	-0.1453759E 06
			0.1037E-04	0.5109E-04				
4	0.3050E 03	-0.4014E 05	-0.1192E-04	-0.1160E 02	-0.1887E 00	0.2434E-02	0.3048262E 03	-0.4015251E 05
			-0.3092E-05	-0.4703E-04				
5	0.1256E 03	-0.1653E 05	-0.4907E-05	-0.8668E 01	-0.1887E 00	0.3015E-02	0.1254375E 03	-0.1653932E 05
			0.1479E-04	0.1417E-03				
6	0.6362E 02	-0.8370E 04	-0.2485E-05	-0.6922E 01	-0.1887E 00	0.3596E-02	0.6342633E 02	-0.8377289E 04
			0.2371E-04	0.2348E-03				
7	0.3660E 02	-0.4815E 04	-0.1429E-05	-0.5763E 01	-0.1886E 00	0.4176E-02	0.3640651E 02	-0.4820750E 04
			0.8236E-05	0.8110E-04				
8	0.2296E 02	-0.3021E 04	-0.8968E-06	-0.4937E 01	-0.1886E 00	0.4756E-02	0.2277415E 02	-0.3026202E 04
			0.7722E-05	0.7604E-04				
9	0.1535E 02	-0.2019E 04	-0.5994E-06	-0.4318E 01	-0.1886E 00	0.5337E-02	0.1515886E 02	-0.2023591E 04
			0.1062E-04	0.1055E-03				
10	0.1076E 02	-0.1416E 04	-0.4203E-06	-0.3837E 01	-0.1886E 00	0.5917E-02	0.1057331E 02	-0.1419771E 04
			0.2914E-05	0.2858E-04				
11	0.7836E 01	-0.1031E 04	-0.3060E-06	-0.3453E 01	-0.1885E 00	0.6497E-02	0.7647958E 01	-0.1034482E 04
			0.4233E-04	0.4216E-03				
12	0.5883E 01	-0.7740E 03	-0.2297E-06	-0.3138E 01	-0.1885E 00	0.7077E-02	0.5694139E 01	-0.7771033E 03
			0.5497E-05	0.5501E-04				
13	0.4528E 01	-0.5958E 03	-0.1768E-06	-0.2877E 01	-0.1885E 00	0.7656E-02	0.4339760E 01	-0.5986414E 03
			0.3726E-05	0.3409E-04				
14	0.3560E 01	-0.4684E 03	-0.1390E-06	-0.2655E 01	-0.1884E 00	0.8236E-02	0.3371421E 01	-0.4710093E 03
			0.9864E-05	0.9881E-04				
15	0.2849E 01	-0.3748E 03	-0.1113E-06	-0.2465E 01	-0.1884E 00	0.8815E-02	0.2660693E 01	-0.3773052E 03
			0.3795E-05	0.3776E-04				
16	0.2316E 01	-0.3047E 03	-0.9043E-07	-0.2301E 01	-0.1884E 00	0.9394E-02	0.2127314E 01	-0.3069585E 03
			0.3862E-05	0.3826E-04				
17	0.1908E 01	-0.2510E 03	-0.7449E-07	-0.2157E 01	-0.1883E 00	0.9973E-02	0.1719237E 01	-0.2531191E 03
			0.5980E-05	0.5903E-04				
18	0.1590E 01	-0.2092E 03	-0.6209E-07	-0.2030E 01	-0.1883E 00	0.1055E-01	0.1401714E 01	-0.2112092E 03
			0.6598E-05	0.6837E-04				
19	0.1339E 01	-0.1762E 03	-0.5230E-07	-0.1917E 01	-0.1882E 00	0.1113E-01	0.1159984E 01	-0.1781004E 03
			0.1300E-04	0.1288E-03				
20	0.1137E 01	-0.1498E 03	-0.4446E-07	-0.1816E 01	-0.1882E 00	0.1171E-01	0.9593471E 00	-0.1515951E 03
			0.1088E-04	0.1097E-03				
21	0.9760E 00	-0.1284E 03	-0.3811E-07	-0.1725E 01	-0.1881E 00	0.1229E-01	0.7878837E 00	-0.1301222E 03
			0.7207E-05	0.6875E-04				

TABLE 11.

ELECTRIC FIELD CALCULATIONS FOR H = 1, k_o = .1, a = $\frac{1}{250}$, X = 2., Y^2 = 2., Z = .05

FIELD ELEMENTS NO.	EZS		EZPS1/EZPS2		EZP		SUM	
1	-0.1240E 06	0.1229E 07	0.1015E 03	-0.1915E 03	-0.4534E 00	-0.3043E 00	-0.1238411E 06	0.1228670E 07
			0.4989E 02	-0.6250E 00				
2	0.5523E 05	-0.5467E 06	0.1737E-01	-0.3799E 02	-0.4574E 00	-0.2997E 00	0.55227C9E 05	-0.5467021E 06
			0.1079E-03	-0.1149E 00				
3	0.4335E 04	-0.4329E 05	0.1381E-02	-0.1763E 02	-0.4613E 00	-0.2951E 00	0.4334813E 04	-0.4340444E 05
			0.1240E-05	-0.9211E-02				
4	0.1192E 04	-0.1194E 05	0.3803E-03	-0.1161E 02	-0.4651E 00	-0.2904E 00	0.1191824E 04	-0.1195636E 05
			0.3511E-06	-0.2535E-02				
5	0.4904E 03	-0.4914E 04	0.1565E-03	-0.8671E 01	-0.4685E 00	-0.2857E 00	0.4899182E 03	-0.4923238E 04
			0.7980E-06	-0.1034E-02				
6	0.2482E 03	-0.2487E 04	0.7520E-04	-0.6924E 01	-0.4726E 00	-0.2809E 00	0.2477026E 03	-0.2494569E 04
			0.9947E-06	-0.5194E-03				
7	0.1427E 03	-0.1431E 04	0.4555E-04	-0.5764E 01	-0.4762E 00	-0.2760E 00	0.1422423E 03	-0.1436563E 04
			0.8956E-06	-0.2960E-03				
8	0.8954E 02	-0.8979E 03	0.2859E-04	-0.4937E 01	-0.4798E 00	-0.2711E 00	0.8905067E 02	-0.9027046E 03
			-0.1074E-05	-0.1999E-03				
9	0.5984E 02	-0.5998E 03	0.1910E-04	-0.4318E 01	-0.4833E 00	-0.2662E 00	0.5935201E 02	-0.6043796E 03
			0.1254E-05	-0.1157E-03				
10	0.4195E 02	-0.4206E 03	0.1339E-04	-0.3837E 01	-0.4867E 00	-0.2612E 00	0.4146703E 02	-0.4246553E 03
			-0.2493E-06	-0.9222E-04				
11	0.3055E 02	-0.3062E 03	0.9750E-05	-0.3453E 01	-0.4901E 00	-0.2562E 00	0.3005763E 02	-0.3099331E 03
			0.5731E-06	-0.6232E-04				
12	0.2293E 02	-0.2299E 03	0.7319E-05	-0.3139E 01	-0.4933E 00	-0.2511E 00	0.2243727E 02	-0.2332566E 03
			-0.8090E-06	-0.5639E-04				
13	0.1765E 02	-0.1769E 03	0.5634E-05	-0.2877E 01	-0.4966E 00	-0.2460E 00	0.1715382E 02	-0.1800602E 03
			-0.1174E-05	-0.5017E-04				
14	0.1388E 02	-0.1391E 03	0.4429E-05	-0.2655E 01	-0.4997E 00	-0.2409E 00	0.1337588E 02	-0.1419528E 03
			0.1654E-05	-0.9415E-05				
15	0.1116E 02	-0.1113E 03	0.3545E-05	-0.2465E 01	-0.5027E 00	-0.2357E 00	0.1060203E 02	-0.1140229E 03
			0.3855E-06	-0.2239E-04				
16	0.9026E 01	-0.9048E 02	0.2881E-05	-0.2301E 01	-0.5057E 00	-0.2305E 00	0.9519926E 01	-0.9301060E 02
			-0.1038E-06	-0.2339E-04				
17	0.7435E 01	-0.7453E 02	0.2373E-05	-0.2157E 01	-0.5086E 00	-0.2252E 00	0.6926190E 01	-0.7691434E 02
			0.2512E-06	-0.1138E-04				
18	0.6197E 01	-0.6212E 02	0.1978E-05	-0.2030E 01	-0.5114E 00	-0.2199E 00	0.5685566E 01	-0.6437413E 02
			0.1499E-05	0.3379E-05				
19	0.5220E 01	-0.5232E 02	0.1666E-05	-0.1917E 01	-0.5142E 00	-0.2146E 00	0.4705379E 01	-0.5445650E 02
			0.1350E-06	-0.8402E-05				
20	0.4437E 01	-0.4448E 02	0.1416E-05	-0.1816E 01	-0.5169E 00	-0.2093E 00	0.3920434E 01	-0.4650848E 02
			-0.5612E-06	-0.2038E-04				
21	0.3804E 01	-0.3815E 02	0.1214E-05	-0.1725E 01	-0.5195E 00	-0.2039E 00	0.3284396E 01	-0.4006265E 02
			0.1176E-06	-0.4383E-06				

TABLE 12.

ELECTRIC FIELD CALCULATIONS FOR H = 1., k_o = .1, a = $\frac{1}{250}$, X = 2.5, Y^2 = .5, Z = .05

FIELD ELEMENTS NO.	EZS		EZFS1/EZFS2		EZF		SUM	
1	-0.1687E 06	-0.9006E 06	0.3517E 01	-0.1877E 03	-0.6655E-01	0.5747E 00	-0.1687176E 06	-0.9006663E 06
			0.1992E 01	-0.2402E 02				
2	0.7488E 05	0.3998E 06	0.1302E-01	-0.3780E 02	-0.6537E-01	0.5694E 00	0.7487925E 05	0.3997454E 06
			0.2552E-02	-0.9982E-01				
3	0.6065E 04	0.3227E 05	0.8069E-03	-0.1762E 02	-0.6421E-01	0.5641E 00	0.6065414E 04	0.3225548E 05
			0.2031E-03	-0.8067E-02				
4	0.1673E 04	0.8899E 04	0.2225E-03	-0.1161E 02	-0.6308E-01	0.5590E 00	0.1673019E 04	0.8887973E 04
			0.5510E-04	-0.2228E-02				
5	0.6888E 03	0.3663E 04	0.9156E-04	-0.8665E 01	-0.6196E-01	0.5539E 00	0.6886992E 03	0.3654555E 04
			0.2789E-04	-0.8665E-03				
6	0.3487E 03	0.1854E 04	0.4635E-04	-0.6923E 01	-0.6087E-01	0.5489E 00	0.3486445E 03	0.1848105E 04
			0.1710E-04	-0.4083E-03				
7	0.2006E 03	0.1067E 04	0.2666E-04	-0.5763E 01	-0.5979E-01	0.5439E 00	0.2005141E 03	0.1061442E 04
			0.1147E-04	-0.2189E-03				
8	0.1258E 03	0.6693E 03	0.1673E-04	-0.4937E 01	-0.5874E-01	0.5390E 00	0.1257891E 03	0.6648579E 03
			-0.1602E-05	-0.2260E-03				
9	0.8411E 02	0.4473E 03	0.1118E-04	-0.4318E 01	-0.5770E-01	0.5341E 00	0.8405119E 02	0.4435010E 03
			0.4961E-05	-0.9178E-04				
10	0.5898E 02	0.3136E 03	0.7839E-05	-0.3837E 01	-0.5669E-01	0.5294E 00	0.5891948E 02	0.3103213E 03
			0.4578E-05	-0.5319E-04				
11	0.4294E 02	0.2284E 03	0.5708E-05	-0.3453E 01	-0.5569E-01	0.5246E 00	0.4288834E 02	0.2254427E 03
			0.5575E-05	-0.1654E-04				
12	0.3224E 02	0.1714E 03	0.4285E-05	-0.3138E 01	-0.5472E-01	0.5200E 00	0.3218199E 02	0.1688117E 03
			0.5533E-05	-0.1612E-04				
13	0.2481E 02	0.1320E 03	0.3298E-05	-0.2877E 01	-0.5376E-01	0.5154E 00	0.2476035E 02	0.1295966E 03
			0.2078E-05	-0.1214E-04				
14	0.1954E 02	0.1037E 03	0.2593E-05	-0.2655E 01	-0.5282E-01	0.5108E 00	0.1945451E 02	0.1015925E 03
			0.7449E-05	-0.3082E-04				
15	0.1561E 02	0.8302E 02	0.2075E-05	-0.2465E 01	-0.5189E-01	0.5063E 00	0.1556052E 02	0.8106488E 02
			-0.9174E-06	-0.3896E-04				
16	0.1265E 02	[illegible]	0.1637E-05	-0.2301E 01	-0.5099E-01	0.5019E 00	0.1263827E 02	0.6568045E 02
			[illegible]	0.1185E-04				
17	[illegible]	[illegible]	[illegible]	-0.2157E 01	-0.5010E-01	0.4975E 00	0.1040282E 02	0.5392723E 02
			[illegible]	-0.4145E-04				
18	[illegible]	[illegible]	[illegible]	-0.2020E 01	-0.4922E-01	0.4932E 00	0.8663486E 01	0.4479576E 02
			[illegible]	0.3040E-04				
19	[illegible]	[illegible]	[illegible]	-0.1917E 01	-0.4837E-01	0.4889E 00	0.7290071E 01	0.3759627E 02
			[illegible]	0.2860E-04				
20	[illegible]	[illegible]	[illegible]	-0.1816E 01	-0.4753E-01	0.4847E 00	0.6191108E 01	0.3184439E 02
			[illegible]	0.3607E-04				
21	[illegible]	0.2644E 02	0.7104E-06	-0.1725E 01	-0.4670E-01	0.4806E 00	0.5301460E 01	0.2719563E 02
			[illegible]	-0.4290E-04				

As expected, the impedance matrix Z is best conditioned when it is most nearly diagonal, or when the singular terms which decrease rapidly with distance are dominant over the finite term. For the overdense elliptic plasma which gives good results as compared to Balmain's approximation, the field contribution on a segment distance 2H from the source due to the finite term is two orders of magnitude less than the total field, while for the overdense hyperbolic case $X = 2$, $Y^2 = 2$, which gives negative radiation resistances, the finite term is an order of magnitude larger than the total field. The hypothesis that the difficulties encountered in some regions are due to an incorrect evaluation of the E_{zf} term, either through invalid approximations or poor numerical quadrature, is strengthened by the tendency of results to get worse as k_o increases. In the singular terms, k_o appears only in the coefficient, while in the finite term, k_o is a factor in the neglected terms of a Taylor series. A method is currently being investigated to evaluate fields for which the finite term is significant by an asymptotic expansion of the transformed Green's function.

Calculations were made to test the sensitivity theory discussed in the last chapter. Consistent with the high condition numbers, it was found that a 1 per cent perturbation of the diagonal term in the Z matrix can cause a 30 per cent change of the impedance both for free space and the hyperbolic overdense plasma. One should note that we are unable to obtain the condition number of an error-free matrix. If errors have occurred which make the matrix more diagonal, a deceptively low condition will be calculated. In cases where large error must be present, such as for the overdense hyperbolic plasma, one

cannot claim that the results approximate the true results within definite limits when only the condition number of the matrix with errors is known.

CHAPTER VII. CONCLUSIONS

Using the method of moments we have been able to calculate the current distribution on an antenna oriented parallel to the static magnetic field in a plasma. For most plasma regions, reasonable impedances are obtained that agree with the Balmain approximation when k_o is small. Calculations on the overdense hyperbolic plasma, however, give unrealizable results. The exact cause of this discrepancy is not well understood; work is continuing on a different method of calculating the fields that will be more accurate and faster for segments far from the feed.

A method of quantitatively analyzing the degree of ill-conditioning has been discussed. This method applies not only to this problem but to any application of the method of moments. In particular, it is suggested that the stability of free-space, thin-wire problems be evaluated. This method can also be applied to inversion problems arising from remote sensing studies.

APPENDIX (LISTING OF PROGRAM USED)

```
C  PREPARES E'S TO BE INVERTED
C   LIMITS CHANGES
      COMPLEX E,E1,EZ,EZS,EZFS1,T(55),EZFS2,EZFN1,T1(3025),EZZ,AD,ZIMP,
     1  EZFN2,U,ER(21),Y1(21),THOLD,TEZ(21)
      DIMENSION PM(30),PP(30),ZZ(30),SM(2),PM1(3,30),PP1(3,30)
      REAL SC1(12)/10.,8.,7.5,6.,5.,4.,3.,2.50,2.,1.50,1.,0.5/
      REAL KO/.576/,PER(3)/0.,.01,.1/
      REAL SSS(4)/4.53,5.35,13.47,50./
      REAL SP(2)/-3.,1.50/,K1(3)/.1,0.75,1.5/
      PI=3.141593
      H=1.
      A=1./250.
      CALL CCP1PL(.5,1.,-3)                                          P
C   M IS NUMBER OF SEGNENTS
      B=SQRT(2.)*A
      M=21
      XM=M
      DO 1000 KJOB=1,1
      READ (5,25) XC,YC2,ZC
   25 FORMAT (3F10.6)
      YC=SQRT(YC2)
      SS=0.
      SS1=0.
      NPLOT=3
C        XC,YC, AND ZC ARE 3 PLASMA PARAMETERS (DON'T USE X,Y,Z)
      DL=H/(XM+2.)
      U=(1.,0.)-(0.,1.)*ZC
      E=(1.,0.)-U*XC/(U**2-YC**2)
      E1=YC*XC/(U**2-YC**2)
      E1=E1/E
      EZ=(1.,0.)-XC/U
      EZ=EZ/E
      DO 11 IXX=1,NPLOT
      KO=K1(IXX)
      PRINT 24,KO,U,XC,YC2,ZC,E,E1,EZ,M
   24 FORMAT('1','KO=',F6.3,5X,'U=',2G16.7,5X,'XC=', G16.7,  5X,'YC2=',
     1   G16.7,5X,'ZC=',
     1 G16.7/'0','E=',2G16.7,5X,'E1=',2G16.7,5X,'EZ=',2G16.7,5X,'M=',I4)
      PRINT 4
    4 FORMAT (1H1,'FIELD ELEMENTS'/' NO.',T17,'EZS',T43,'EZFS1/EZFS2',
     1 T75,'EZFN1',T109,'SUM')
C   ECYL FOR EZS, E2DL1 FOR EZFS1
      KK=MIN0(30,M)
      DO 2 I=1,KK
      X=I-1
      Z=X*2.*DL
      CALL E2DL1(KO,E,E1,EZ,B,DL,Z,EZZ,EZFS1,EZFS2)
      CALL ECYL(KO,E,E1,EZ,A,DL,Z,EZS)
      CALL EZFN(KO,E,E1,EZ,DL,Z,    EZFN1,ER(I),Y1(I))
      T(I)=EZS+EZFS1+EZFN1+EZFS2
    2 WRITE (6,51) I,EZS,EZFS1       ,EZFN1,T(I) ,EZFS2
   51 FORMAT (1H ,I3,6E15.4,2E18.7/1H ,33X,2E15.4)
      IF(M .LT. 31) GO TO 12
```

```
C       E2DL1
        KK=MINO(50,M)
        DO 5 I=31,KK
        X=I-1
        Z=X*2.*DL
        CALL E2DL1(KO,E,E1,EZ,B,DL,Z,EZS,EZFS1,EZFS2)
        CALL EZFN(KO,E,E1,EZ,DL,Z,    EZFN1,ER(I),Y1(I))
        T(I)=EZS+EZFS1+EZFN1+EZFS2
      5 WRITE (6,51) I,EZS,EZFS1      ,EZFN1,T(I) ,EZFS2
     12 WRITE (6,104)
    104 FORMAT (1HO,'INTEGRATION AND ERROR'//'NO.',T15,'UNNORMALIZED EZFN1
       1',T56,'ERROR')
        COND=0.
        DO 71 I=1,M
        WRITE (6,3) I,Y1(I),ER(I)
      3 FORMAT (1H ,I3,5X,2E15.7,5X,2F15.7)
        DO 6 J=1,M
        K=M *(I-1)+J
        KK=IABS(J-I) +1
      6 T1(K)=T(KK)
        M1=IABS(M/2+1-I)+1
        COND=COND+CABS(T(M1))
     71 CONTINUE
        WRITE (6,72) COND
     72 FORMAT (1HC,5X,'NORM BEFORE INVERSION =',E16.7)
        CHOLD=COND
        CALL LINEQ(M ,T1)
        IHOLD=0
        CONDIT=0.
        DO 73 I=1,M
        COND=0.
        DO 74 J=1,M
        KK=M*(I-1)+J
     74 COND=COND+CABS(T1(KK))
        IF (COND .LE.CONDIT) GO TO 73
        IHOLD=I
        CONDIT=COND
     73 CONTINUE
        WRITE (6,75) CONDIT,IHOLD
     75 FORMAT (1H ,5X,'NORM AFTER INVERSION  =',E16.7,5X,'ROW',I2)
        COND=COND*CHOLD
        WRITE (6,76) COND
     76 FORMAT (1H ,5X,'ESTIMATE OF CONDITION =' ,E16.7)
        PRINT 7
      7 FORMAT('1')
        KK=M**2 -2
      9 FORMAT(' ',I4,3(5X,2E16.7))
        PRINT 15
     15 FORMAT('0'///' NOT MULT BY -1/(2DL)**2')
        DO 14 I=1,KK,3
     14 PRINT 9,I,T1(I),T1(I+1),T1(I+2)
C
        M2=M**2
```

```
      F=-1./(2.*DL)**2
      DO 13 I=1,M2
   13 T1(I)=F*T1(I)
      MM=((M2-1)/2+1)
      AD=T1(MM)*1000.
      ZIMP=1./T1(MM)
      M1=((M-1)/2) *M
      M3=(M+1)/2
      M4=M1+1
      M5=M1+M3
      DO 17 I=M4,M5
      XX=CABS(T1(I))
      XY=ATAN2(AIMAG(T1(I)),REAL(T1(I)))
   17 T1(I)=CMPLX(XX,XY)
      PRINT 21
   21 FORMAT('0'///' ',10X,'CURRENTS  (MAG AND PHASE)')
      DO 20 I=1,M3
   20 PRINT 22,T1(I+M1)
   22 FORMAT(' ',10X,2G16.7)
      PRINT 23,AD,ZIMP
   23 FORMAT('0'///' ',10X,'ADMITTANCE= ',2G16.7,' MILLIMHOS'/
     1  ' ',10X,'IMPEDANCE= ',2G16.7,' OHMS')
C                START PLOTTING
  100 M4=M3+1
      DO 30 I=1,M3
      PM(I+1)= REAL(T1(I+M1))
      IF (PM(I+1).GT.SS) SS=PM(I+1)
      PM1(IXX,I+1)=-PM(I+1)
      PP(I+1)= AIMAG(T1(I+M1))
   30 PP1(IXX,I+1)=-PP(I+1)
      PM(1)=0.
      PM1(IXX,1)=0.0
      PP(1)=0.
      PP1(IXX,1)=0.
   11 CONTINUE
      SS=SS/4.
      DO 53 K=1,7
      IF (SS.GE.1.) GO TO 54
   53 SS=SS*10.
   54 K=K-1
      DO 55 I=2,12
      IF (SS.GT.SC1(I)) GO TO 56
   55 CONTINUE
   56 SM(2)=SC1(I-1)/10.**K+1.E-6
      SM(1)=0.
C     START PLOTTING
      CALL CCP1BA
      CALL CCP1PL(4.5,2.,-3)
      CALL CCP1PL(0.,0.,3)
      CALL CCP1PL(0.,6.,2)
      CALL FACTOR (.5)
      CALL CCP2SY(-7.8,.5,.3,'H= ',90.,3)
      CALL CCP3NR(0.,0.,-.3,H ,90.,3)
```

```
      CALL CCP2SY(-7.4,.5,.3,'X= ',90.,3)
      CALL CCP3NR(0.,0.,-.3,XC,90.,3)
      CALL CCP2SY (-7.0,.5,.3,'Y 2 =',90.,5)
      CALL CCP3NR(0.,0.,-.3,YC2,90.,3)
      CALL CCP2SY(-6.6,.5,.3,'Z= ',90.,3)
      CALL CCP3NR(0.,0.,-.3,ZC,90.,3)
      YP=.5
      XP=-6.2
      DO 52 K=1,NPLOT
      L=K
      IF (K.EQ.3) L=0
      CALL CCP2SY(XP,YP,.3,'KO=',90.,3)
      CALL CCP3NR (0.,0.,-.3,K1(K),90.,3)
      CALL CCP2SY (0.,0.,-.3,'...',90.,3)
      CALL CCP2SY (0.,0.,-.15,L,90.,-1)
   52 XP=XP+.4
      CALL FACTOR(1.)
      CALL CCP5AX(0.,0.,'MAG OF CURRENT',14,4.000,180.,SM)
      CALL CCP2SY (.3,1.370,.15,'MID POINTS OF SEGMENTS',90.,22)
      CALL CCP2SY (.3,5.800,.15,'FEED',90.,4)
      DO 46 I=1,M4
      XXI=I-1
      ZZ(I)=12./(XM+1.)*XXI
      CALL CCP2SY (0.,ZZ(I),.07,13,90.,-1)
      DO 46 K=1,NPLOT
      L=K
      IF (K.EQ.3) L=0
      PM1(K,I)=(PM1(K,I)+SM(1))/SM(2)
   46 CALL CCP2SY (PM1(K,I),ZZ(I),0.07,L,90.,-1)
      DO 49 K=1,NPLOT
      CALL CCP1PL(PM1(K,1),ZZ(1),3)
      DO 49 I=2,M4
   49 CALL CCP1PL(PM1(K,I),ZZ(I),2)
      CALL CCP1PL(2.5,0.,-3)
      CALL CCP1PL(0.,6.,2)
      CALL CCP5AX(2.000,0.,'PHASE OF CURRENT',16,4.000,180.,SP)
      CALL CCP2SY (.3,1.370,.15,'MID POINTS OF SEGMENTS',90.,22)
      CALL CCP2SY (.3,5.800,.15,'FEED',90.,4)
      DO 47 I=2,M4
      CALL CCP2SY(0.,ZZ(I),.07,13,90.,-1)
      DO 47 K=1,NPLOT
      L=K
      IF (K.EQ.3) L=0
      PP1(K,I)=(      PP1(K,I))/SP(2)
   47 CALL CCP2SY(PP1(K,I),ZZ(I),0.07,L ,90.,-1)
      DO 50 K=1,NPLOT
      CALL CCP1PL(PP1(K,2),ZZ(2),3)
       DO 50 I=3,M4
   50 CALL CCP1PL(PP1(K,I),ZZ(I),2)
      CALL CCP1PL(4.,-2.,-3)
 1000 CONTINUE
      CALL EXIT
      END
```

```
      SUBROUTINE LINEQ(LL,C)
C      2/5/71 C KLEIN CHANGED ARITH IFS TO LOGICAL IFS
      COMPLEX C(1),STOR,STO,ST,S
      DIMENSION LR(58)
      DO 20 I=1,LL
      LR(I)=I
   20 CONTINUE
      M1=0
      DO 18 M=1,LL
      K=M
      DO 2 I=M,LL
      K1=M1+I
      K2=M1+K
      IF ((CABS(C(K1))-CABS(C(K2))) .LE. 0.) GO TO 2
    6 K=I
    2 CONTINUE
      LS=LR(M)
      LR(M)=LR(K)
      LR(K)=LS
      K2=M1+K
      STOR=C(K2)
      J1=0
      DO 7 J=1,LL
      K1=J1+K
      K2=J1+M
      STO=C(K1)
      C(K1)=C(K2)
      C(K2)=STO/STOR
      J1=J1+LL
    7 CONTINUE
      K1=M1+M
      C(K1)=1./STOR
      DO 11 I=1,LL
      IF(I-M) 12,11,12
   12 K1=M1+I
      ST=C(K1)
      C(K1)=0.
      J1=0
      DO 10 J=1,LL
      K1=J1+I
      K2=J1+M
      C(K1)=C(K1)-C(K2)*ST
      J1=J1+LL
   10 CONTINUE
   11 CONTINUE
      M1=M1+LL
   18 CONTINUE
      J1=0
      DO 9 J=1,LL
      IF(J-LR(J) .EQ. 0) GO TO 8
   14 LRJ=LR(J)
      J2=(LRJ-1)*LL
   21 DO 13 I=1,LL
```

```
      K2=J2+I
      K1=J1+I
      S=C(K2)
      C(K2)=C(K1)
      C(K1)=S
   13 CONTINUE
      LR(J)=LR(LRJ)
      LR(LRJ)=LRJ
      IF(J-LR(J) .NE. 0) GO TO 14
    8 J1=J1+LL
    9 CONTINUE
      RETURN
      END
```

```
      SUBROUTINE EZFN(KO,E,E1,EZ,DL,Z,EZFN1,ERROR,Y1)
      REAL KO
      REAL*8 XY/1D0/
      COMPLEX E,E1,EZ,X,EZFN1,ERROR,Y1
      REAL* 8 P12/1.5707963268/
      COMPLEX *16 Y,DAPHI1,DAPHI0,DHPHI2,ERR
      X=DHPHI0(DBLE(KO),DCMPLX(DBLE(REAL(E )),DBLE(AIMAG(E))),
     1                  DCMPLX(DBLE(REAL(E1)),DBLE(AIMAG(E1))),
     2                  DCMPLX(DBLE(REAL(EZ)),DBLE(AIMAG(EZ))),
     3DBLE(DL),DBLE(Z))
      CALL ROMBRG(0D0,P12,DAPHI1,8,Y,1D-4,1D-3,ERR)
      ERROR=ERR
      Y1=Y
      K=DREALZ(DHPHI2(XY))
      X=Y
      EZFN1=(0.,15.)*KO**2*X
      RETURN
      END
```

```
      SUBROUTINE E2DL1 (KO,E,E1,EZ,A,DL,Z,EZS,EZFS1,EZFS2)
C       THIS SUBROUTINE CALCULATES FIRST THREE E TERMS USING 2 DL MODEL
      COMPLEX E,E1,EZ,EZS,EZFS1,EZFS2,A12,ZAP,ZAM,ZAPH,ZAMH,ZF2,ZF3
C    RETURNS COMPLEX NUMBERS
C   THIS REPLACES SUBROUTINE E2DL
      REAL KO
      A12=EZ*A**2
      ZPDL=Z+DL
      ZMDL=Z- DL
      ZPDL2=ZPDL**2
      ZMDL2=ZMDL**2
      ZAP = ZPDL**2 +A12
      ZAM=ZMDL  **2 +A12
      ZAPH=CSQRT(ZAP)
      ZAMH=CSQRT(ZAM)
      ZF2=CLOG((ZPDL+ZAPH)/(ZMDL+ZAMH))
      ZF3=ZPDL /ZAPH - ZMDL/ZAMH
C       EZS SIMPLIFIED 2/7/70
      EZS=(0.,15.)/(KO*DL*E)*(ZPDL/(ZAP*ZAPH)-ZMDL/(ZAM*ZAMH))
      EZFS1=(0.,-7.5)*(KO/DL)*((2.,0.)*ZF2-ZF3)
      IF ( REAL(EZ) .NE. 1. .OR. AIMAG(EZ) .NE. 0.  .OR. REAL (E1)
     1  .NE. 0. .OR. AIMAG(E1) .NE. 0.) GO TO 1
      EZFS2= (0.,0.)
      GO TO 2
    1 T1=ALOG ((ZPDL+SQRT(ZPDL2+A**2))/(ZMDL+SQRT(ZMDL2+A**2)))
      EZFS2 =(0.,15.)*E1**2/(EZ-(1.,0.))**2*(KO/DL)*(T1+ZF2*(.5,0.)
     1 ( -2.,0.)+ZF3*(.5,0.)*((1.,0.)-EZ))
C     1      (1.- EZ))
    2 RETURN
      END
```

```
      SUBROUTINE ECYL(KO,E,E1,EZ,A,DL,Z,EZS)
C     THIS EVALUATES EZS USING ELLIPTICAL INTEGRALS
      COMPLEX E,E1,EZ,EZS,X,A12,KP2,KM2
      REAL KO
C     THIS FUNCTION STATEMENT EVALUATES ELLIPTICAL INTEGRAL
      EL(X)=((((A4*X+A3)*X +A2)*X+A1)*X+1.)
     1   -((((B4*X+B3)*X +B2)*X +B1)*X)*CLOG(X)
      DATA A1,A2,A3,A4/.4432514,6.260601E-2,4.757384E-2,1.736506E-2/
      DATA B1,B2,B3,B4/.2499837,9.200180E-2,4.069698E-2,5.264496E-3/
      ZPDL=Z+DL
      ZMDL=Z-DL
      A12=EZ*A**2
      KP2=4.*A12/(ZPDL**2+4.*A12)
      KM2=4.*A12/(ZMDL**2+4.*A12)
      EZS=(0.,15.)/((KO*3.141593*DL*A)*E*CSQRT(EZ))*
     1  (CSQRT(KP2)*EL((1.,0.)-KP2)/ZPDL-
     2   CSQRT(KM2)*EL((1.,0.)-KM2)/ZMDL)
      RETURN
      END
```

```
      SUBROUTINE ROMBR G(A,B,TTT,NMIN,Y,TR,HMIN,ERR)
C       CONVERTED TO COMPLEX
      IMPLICIT COMPLEX*16(A-G,O-W,Y-Z)
      IMPLICIT REAL*8(H,X)
      REAL *8 TR,A,B,DREALZ,DIMAGZ
C  TNT MUST BE DECLARED EXTERNAL IN CALLING PROGRAM
C ADAPTIVE INTERVAL ROMBERG INTEGRATION ROUTINE
C  NMIN IS MIN NUMBER OF SUBINTERVALS
      DIMENSION FF2(10),FF4(10),HF(10)
      NSUB=10
      KODE=0
      HMAX=(B-A)/NMIN
      ERR=( 0D0,0D0)
      Y=(0D0,0D0)
      X4=A
      F4=TNT(A)
      DO 1 JJ=1,NMIN
C  INITIALIZE LARGEST INTERVAL POSSIBLE
       X0=X4
      F0=F4
      X4=X0+HMAX
      F4=TNT(X4)
      X2=X0+.5*HMAX
      LEVEL=0
      F2=TNT(X2)
      H=HMAX
C     START LOOP
    4 W=F0+F4
C     H FACTORED OUT OF T(N,M) TERMS
      T00=W/2D0
      WW=W+2D0*F2
      T01=WW/4D0
      T10=(4D0*T01-T00)/3D0
      IF (DREALZ(T10) .EQ.0.0D0) GO TO 20
      IF(DMAX1  (DABS((DREALZ(T10)-DREALZ(T01))/DREALZ(T10)),
     1            DABS((DIMAGZ(T10)-DIMAGZ(T01))/DIMAGZ(T10))) .LE.
     2      TR) GO TO 8
      GO TO 21
   20 IF (DABS((DIMAGZ(T10)-DIMAGZ(T01))/DIMAGZ(T10)).LE.TR) GO TO 8
   21 CONTINUE
      F1=TNT(X0+.25*H)
      F3=TNT(X4-.25*H)
      T02=(WW+2D0*(F1+F3))/8D0
      T11=(4D0*T02-T01)/3D0
      T20=(16D0*T11-T10)/15D0
      IF (DREALZ(T20) .EQ.0.0D0) GO TO 22
      IF(DMAX1(  DABS((DREALZ(T20)-DREALZ(T11))/DREALZ(T20)),
     1   DABS((DIMAGZ(T20)-DIMAGZ(T11))/DIMAGZ(T11)))
     2   .LE. TR) GO TO 2
      GO TO 23
   22 IF (DABS((DIMAGZ(T20)-DIMAGZ(T11))/DIMAGZ(T11)).LE.TR) GO TO 2
   23 CONTINUE
      IF (LEVEL .LT. NSUB .AND. H .GT.HMIN) GO TO 3
```

```
      KODE=1
      GO TO 2
C      SUBDIVIDE
    3 H=H/2.
      LEVEL=LEVEL+1
      FF2(LEVEL)=F3
      HF(LEVEL)=H
      FF4(LEVEL)=F4
      F4=F2
      F2=F1
      X4=X0+H
      GO TO 4
    8 Y=Y+T10*H
      ERR=ERR+(T10-T01)*H
      GO TO 9
C     UNSUBDIVIDE
    2 Y=Y+T20*H
      ERR=ERR+(T20-T11)*H
    9 IF(LEVEL .EQ. 0) GO TO 1
      F0=F4
      F2=FF2(LEVEL)
      F4=FF4(LEVEL)
      H=HF(LEVEL)
      X0=X4
      X4=X0+H
      LEVEL=LEVEL-1
      GO TO 4
    1 CONTINUE
      IF(KODE .EQ. 1) PRINT 5
    5 FORMAT(' ACCURACY SPECIFIED CANNOT BE OBTAINED')
      RETURN
      END
```

```
      COMPLEX FUNCTION DHPHI0*16(K0,E,E1,EZ,DL,Z)
      IMPLICIT REAL*8(A-H,O-Z)
C     EXTENSIVE CHANGES 7-28-71  TWO INTEGRAND HALVES SUMMED AND COUNTER
C        FOR TIMES CALLED ADDED
C      CHANGES MADE 5/1/71 HC ELIMINATED AND INCLUDED IN HPHI
C     CHANGES MADE 4/20/71 ABOUT SQRT OF N1
C        DON'T DO UNIAXIAL CASE
C      CHANGES MADE 4/15/71 HPHI NO LONGER NEEDS HCEO
      COMPLEX*16 N1,U1,U2,COEF,H,E1,EZ,E,N12,ST,DSCR,N22,DUM,E12,A,B,C,
     1   H1,D1,TNT,DHPHI2
      REAL*8 K0
      I=0
      DHPHI0=(0D0,0D0)
      RETURN
      ENTRY TNT(PHI)
      I=I+1
      SP=DSIN(PHI)
      SP2=SP**2
      CP=DCOS(PHI)
      IF( CDABS(E1) .EQ. 0D0) GO TO 1
C  H FOR E1 ¬=0
      E12=E1**2
      CP2=CP**2
      A=SP2+EZ*  CP2
      B=EZ*(1D0+CP2)+(1D0-E12)*SP2
      C=(1D0-E12)*EZ
      DSCR=CDSQRT(B**2-4D0*A*C)
      N12=(B-DSCR)/(2D0*A)
      N22=(B+DSCR)/(2D0*A)
      DUM=(0D0,-2D0)*SP*SP2/(A**2*(N12-N22))
      D1=1D0+E12*CP2
      H=DUM*(1D0-E12-N12*D1)
      H1=-DUM*(1D0-E12-N22*D1)
      GO TO 2
C     H FOR E1=0
    1 N12=(1D0,0D0)
      N22=N12
      H=(0D0,2D0)*SP*SP2
      H1=(0D0,0D0)
C  CALCULATING SIN(  )/ (  ) TERM
    2 ST=CDSQRT(N12*E)
      IF(DIMAGZ(ST) .GT. 0D0) ST=-ST
      U1=(ST*K0*CP)
      U2=U1*DL
      IF (              CDABS(U2).LT. 1.D-3) GO TO 3
      COEF=CDSIN(U2)/U2
      GO TO 4
    3 COEF=(1D0,0D0)
    4 TNT  =H*CDEXP(-(0D0,1D0)*U1*DABS(Z))*COEF*ST
      ST=CDSQRT(N22*E)
      IF(DIMAGZ(ST) .GT. 0D0) ST=-ST
      U1=(ST*K0*CP)
      U2=U1*DL
```

```
      IF (                CDABS(U2).LT. 1.D-3) GO TO 6
      COEF=CDSIN(U2)/U2
      GO TO 8
    6 COEF=(1D0,0D0)
    8 TNT=H1* CDEXP(-(0D0,1D0)*U1*DABS(Z))*COEF*ST+TNT
    9 RETURN
      ENTRY DHPHI2(X)
      DHPHI2=DCMPLX(DBLE(FLOAT(I)),0D0)
      RETURN
      END
```

REFERENCES

[1] R. Mittra and G. A. Deschamps, "Field solution for a dipole in an anisotropic medium," Symposium on Electromagnetic Theory and Antennas — Copenhagen, June 25 - 30, 1962. New York: Pergamon Press, 1963, pp. 495-512.

[2] A. Erdélyi, W. Magnus, F. Oberhettinger, and F. G. Tricomi, Higher Transcendental Functions, vol. II. New York: McGraw-Hill, 1953, p. 26.

[3] Ibid., p. 33.

[4] H. B. Dwight, Tables of Integrals and Other Mathematical Data. New York: Macmillan, 1961, p. 16.

[5] A. Erdélyi, op cit., p. 81.

[6] R. F. Harrington, Field Computation by Moment Methods. New York: Macmillan, 1968.

[7] E. C. Jordan, Electromagnetic Waves and Radiating Systems. New York: Prentice-Hall, 1950, p. 361.

[8] I. S. Gradshteyn and I. W. Ryzhik, Table of Integrals, Sines and Products. New York: Academic Press, 1965, p. 252.

[9] F. S. Acton, Numerical Methods that Work. Evanston: Harper and Row, 1970.

[10] E. K. Miller and G. J. Burke, "Numerical integration methods," IEEE Trans. Antennas and Propagation (Communications), vol. AP-17, pp. 669-672, September 1969.

[11] G. E. Forsythe and C. B. Moler, Computer Solution of Linear Algebraic Systems. Englewood Cliffs, New Jersey: Prentice-Hall, 1967.

[12] V. N. Faddeeva, Computational Methods of Linear Algebra (translated by C. D. Benster from the Russian book of 1950). New York: Dover Publications, 1959, pp. 54-62.

[13] G. A. Deschamps, "Angular dependence of the refractive index in the ionosphere," J. Res. Natl. Bur. Std. (U.S.), vol. 69D, no. 3, pp. 395-400, March 1965.

[14] K. G. Balmain, "The impedance of a short dipole antenna in a magneto-plasma," IEEE Trans. Antennas and Propagation, vol. AP-12, pp. 605-617.

[15] R. F. Harrington and J. Mautz, "Computations for linear wire antennas and scatterers," Rome Air Development Center, Griffiss Air Force Base, New York, AD639745, Technical Report RADC-TR-66-351, vol. II, 1966.

[16] P. W. Klock, Private Communications.

[17] D. E. Snyder and R. Mittra, "Experimental study of the impedance of a short dipole in a plasma for parallel and perpendicular orientation with respect to the D.C. magnetic field," Antenna Laboratory Report No. 68-4, Antenna Laboratory, University of Illinois, Urbana, Illinois, December 1968.

[18] T. Ishizone, S. Adachi, K. Taira, Y. Mushiake, and K. Miyazaki, "Measurement of antenna current distribution in an anisotropic plasma," IEEE Trans. Antennas and Propagation (Communications), vol. AP-17, pp. 678-679, September 1969.

UNCLASSIFIED
Security Classification

DOCUMENT CONTROL DATA - R & D

(Security classification of title, body of abstract and indexing annotation must be entered when the overall report is classified)

1. ORIGINATING ACTIVITY *(Corporate author)*
Department of Electrical Engineering
University of Illinois
Urbana, Illinois 61801

2a. REPORT SECURITY CLASSIFICATION

2b. GROUP

3. REPORT TITLE
CURRENT DISTRIBUTION ON A CYLINDRICAL ANTENNA WITH PARALLEL ORIENTATION IN A LOSSY MAGNETOPLASMA

4. DESCRIPTIVE NOTES *(Type of report and inclusive dates)*
Scientific-July 1972

5. AUTHOR(S) *(First name, middle initial, last name)*
Charles A. Klein
Paul W. Klock
Georges A. Deschamps

6. REPORT DATE
July 1972

7a. TOTAL NO. OF PAGES
105

7b. NO. OF REFS
18

8a. CONTRACT OR GRANT NO
NGR-14-005-009

b. PROJECT NO.

c.

d.

9a. ORIGINATOR'S REPORT NUMBER(S)
Antenna Laboratory Report No. 72-3
Technical Report No. 19

9b. OTHER REPORT NO(S) *(Any other numbers that may be assigned this report)*
UILU-ENG-72-2546

10 DISTRIBUTION STATEMENT
Unlimited

11. SUPPLEMENTARY NOTES

12. SPONSORING MILITARY ACTIVITY
National Aeronautics and Space Administration

13. ABSTRACT

The current distribution and impedance of a thin cylindrical antenna with parallel orientation to the static magnetic field of a lossy magnetoplasma is calculated with the method of moments. The electric field produced by an infinitesimal current source is first derived. Results are presented for a wide range of plasma parameters. Reasonable answers are obtained for all cases except for the overdense hyperbolic case. A discussion of the numerical stability is included which not only applies to this problem but to other applications of the method of moments.

DD FORM 1 NOV 65 1473

UNCLASSIFIED
Security Classification

14. KEY WORDS	LINK A		LINK B		LINK C	
	ROLE	WT	ROLE	WT	ROLE	WT
Plasma						
Anisotropic Plasma						
Cylindrical Antenna						
Method of Moments						
Stability						
Antenna Impedance						